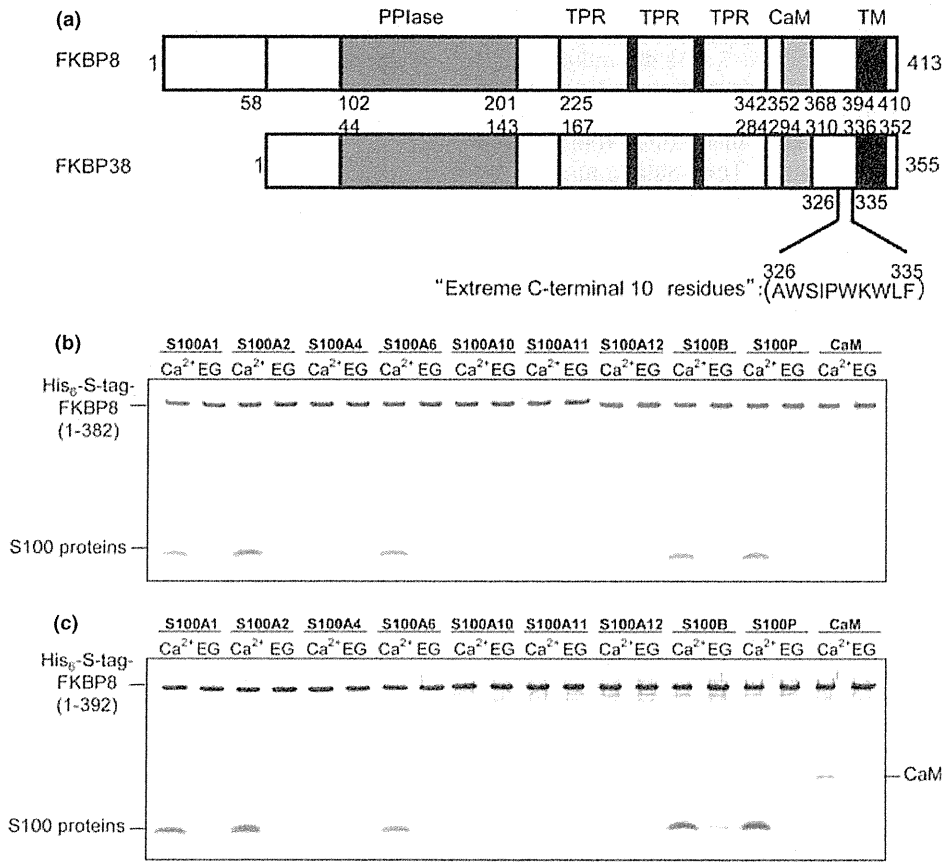

Fig. 1. Interaction of FKBP8 and S100 proteins. (a) Schematic representation of FKBP8 and FKBP38. The peptidyl prolyl *cis/trans* isomerases (PPIase), tetratricopeptide repeat (TPR), calmodulin-binding site (CaM), 'extreme C-terminal 10 residues' and transmembrane domain (TM) are shown. The number refers to the amino acid positions of FKBP8. (b) The S-tag pull-down assay was performed using His_6-S-tag-FKBP8 (1–382) and the S100 proteins. (c) The S-tag pull-down assay was performed using His_6-S-tag-FKBP8 (1–392) and the S100 proteins. The His_6-S-tag-FKBP8 (20 μg) and S100 proteins (20 μg) were incubated with S-protein agarose beads in the presence of either 1 mM $CaCl_2$ or EGTA for 1 h. Beads were washed and samples were separated with 10% Tricine–SDS-PAGE and stained with Coomassie Blue.

Ca^{2+}/CaM-binding site, we prepared a recombinant His_6-S-tag-FKBP8 (1–382) and a His_6-S-tag-FKBP8 (1–392). A precise analysis of the S100 proteins–FKBP38 binding will be described elsewhere (S. Shimamoto, H. Tokumitsu, M. Tsuchiya, Y. Kubota and R. Kobayashi, unpublished data). To test the direct binding of the S100 proteins to FKBP8, we performed a pull-down assay using the S100 proteins with His_6-S-tag-FKBP8 (1–382) or His_6-S-tag-FKBP8 (1–392) in the presence of 1 mM $CaCl_2$ or EGTA. The bound proteins were analysed using Tricine–SDS-PAGE. As shown in Figure 1b, c, S100A1, S100A2, S100A6, S100B and S100P bound strongly to His_6-S-tag-FKBP8 (1–382) or His_6-S-tag-FKBP8 (1–392) in a Ca^{2+}-dependent manner, whereas CaM did not bind to His_6-S-tag-FKBP8 (1–382). In addition, S100A4, S100A10 and S100A11 bound weakly to His_6-S-tag-FKBP8 (1–392).

To examine the real-time binding kinetics of S100A1, S100A2, S100A6, S100B, S100P and CaM to FKBP8, the recombinant His_6-S-tag-FKBP8 (1–392) was immobilized on a sensor chip surface and the protein complex formation was analysed using SPR (Fig. 2a). The binding curves of S100A1, S100A2, S100A6, S100B and S100P were fit to the 1:2 ligand-binding model, whereas the binding curve of CaM was fit to the 1:1 ligand-binding model. The association rate constant (Ka) of S100A1, S100B and S100P to the immobilized FKBP8 (1–392) is indistinguishable and the association of S100A6 and S100A2 occurred more slowly compared with that of other S100 proteins. This suggested an underlying interaction mechanism that was different among the S100 proteins (S100A1, S100B, S100P vs. S100A2, S100A6) (Fig. 2b). The binding concentration of the S100 proteins was measured using a sensorgram. The resonance unit (RU) correlates with the amount of analyte bound (1 RU = 1 pg/mm^2), and the amount of the S100 proteins and CaM binding to FKBP8 (1–392) were significantly different

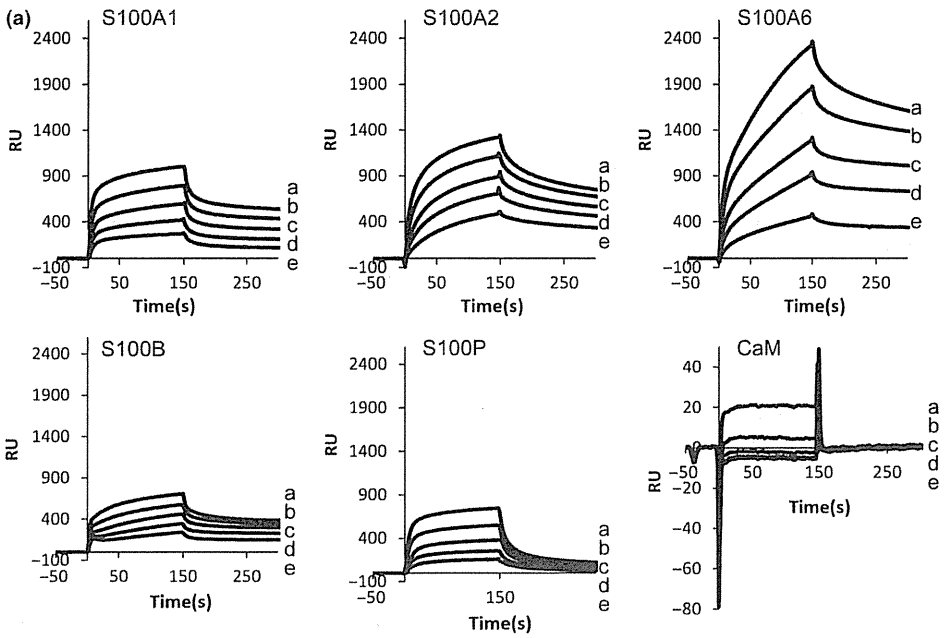

(b) The binding affinity of FKBP8 and S100 protein as analyzed by the Biacore

Analyte	ka1 (1/Ms)	kd1 (1/s)	ka2 (1/Ms)	kd2 (1/s)	KA1 (1/M)	KA2 (1/M)	KD1(M)	KD2 (M)
S100A1	1.08×10^{5}	0.98×10^{-4}	0.38×10^{5}	0.16×10^{-4}	1.11×10^{8}	0.2×10^{10}	9.03×10^{-9}	4.19×10^{-10}
S100A2	0.90×10^{5}	7.15×10^{-4}	0.61×10^{5}	0.08×10^{-4}	0.13×10^{8}	0.73×10^{10}	0.79×10^{-9}	1.37×10^{-10}
S100A6	0.68×10^{5}	5.31×10^{-4}	0.15×10^{5}	0.12×10^{-4}	1.29×10^{8}	0.13×10^{10}	7.76×10^{-9}	7.78×10^{-10}
S100B	5.47×10^{5}	1.17×10^{-4}	2.60×10^{5}	0.27×10^{-4}	4.68×10^{8}	0.97×10^{10}	2.14×10^{-9}	1.03×10^{-10}
S100P	1.21×10^{5}	1.60×10^{-4}	1.99×10^{5}	0.08×10^{-4}	0.76×10^{8}	2.45×10^{10}	0.13×10^{-9}	0.41×10^{-10}
CaM	0.36×10^{5}	0.10×10^{-4}			3.53×10^{8}		2.83×10^{-9}	

Fig. 2. Analysis of FKBP8 and S100 protein binding by *Surface Plasmon Resonance (SPR).* (a) Recombinant His_6-S-tag-FKBP8 was immobilized to the dextran surface of the CM5 chip in 20 mM ammonium acetate, pH 4.2, until 4540 response units (0.3 pmol) were bound and a stable base line was obtained. Recombinant S100A1, S100A2, S100A6, S100B, S100P, S100A12 and CaM were injected at various concentrations (a: 1.25 μM, b: 625 nM, c: 313 nM, d: 156 nM and e: 78 nM). The response curves were prepared for fitting by subtraction of the signal generated simultaneously on the control flow cell. (b) Biacore sensorgram curves were evaluated using BIAevaluation 3.0 using a 1:1 Langmuir model (for CaM) or 1:2 binding model (for the S100 proteins). The calculated kinetic parameters of S100 protein binding to FKBP8 were presented.

(S100A6 > S100A2 > S100A1 ≥ S100P > S100B >> CaM) (Fig. 2).

S100 protein binding to FKBP38

Previous co-immunoprecipitation studies indicated that both NS5A and Hsp90 bound to the TPR domain of FKBP8 and that the interaction between NS5A and FKBP8 did not affect complex formation with Hsp90 (11, 12). Hsp90 has been reported to bind to the two-carboxylate clamp positions within the TPR domain of FKBP8/FKBP38 through its EEVD motif (11, 29), whereas NS5A binds to the FKBP8-TPR through its Val/Ile^{121} residue (12). To define the binding domain of the S100 proteins in FKBP38, the various length FKBP38 and point mutants fused with S-tagged FKBP38 (1–166), FKBP38 (1–297), FKBP38 (1–315), FKBP38 (1–325), FKBP38 (1–335) and KR (where the

250 Lys, 254 Arg in the TPR domain were replaced with Ala) were constructed (Fig. 3a). Each mutant protein was incubated with S100A1, S100A2, S100A6, S100B, S100P, CaM, Hsp90 and NS5A. NS5A and all the S100 proteins bound to all the FKBP 38 truncation mutants and the KR mutant, but did not bind to FKBP38 (1–166) (Fig. 3b). These data indicate that the S100 proteins interact with the C-terminal portion [including TPR and putative CaM-binding domain) of FKBP38 and do not interact with the FK506-binding domain (i.e. FKBP38 (1–166)] (Fig. 3b). In contrast, the last 10 C-terminus residues of FKBP38 are required for the binding of CaM, and the two-carboxylate clamp is essential for the binding of Hsp90. Taken together, these observations prove the direct interaction of NS5A, Hsp90 and the S100 proteins with FKBP38 and imply the existence of similar, but not identical, binding sites of the S100 proteins, NS5A and Hsp90 within FKBP38.

S100 proteins interfere with the interactions of TPR-mediated FKBP8/FKBP38–HSP90 and FKBP8/FKBP38–NS5A

To study whether S100 proteins interfere with the binding of Hsp90 and NS5A to FKBP8/FKBP38, we performed competitive pull-down assays. Fixed amounts of His_6-S-tag-FKBP8/FKBP38 (25 μg) and Hsp90 (25 μg) were mixed with an increasing amount of the S100 proteins (0–50 μg), and a S-tag pull-down was performed (Fig. 4). SDS-PAGE gels demonstrate the displacement effect of the S100 proteins on the FKBP8–Hsp90 (Fig. 4a) and FKBP38–Hsp90 interactions (Fig. 4b). Furthermore, increasing the amount of the S100 proteins (S100A1, S100A2, S100A6, S100B and S100P) strongly inhibited the binding of His_6-S-tag-FKBP8/FKBP38 with Hsp90, whereas a weaker inhibition was detected with CaM. A significant inhibition was not observed with S100A12 as a negative control. To prove

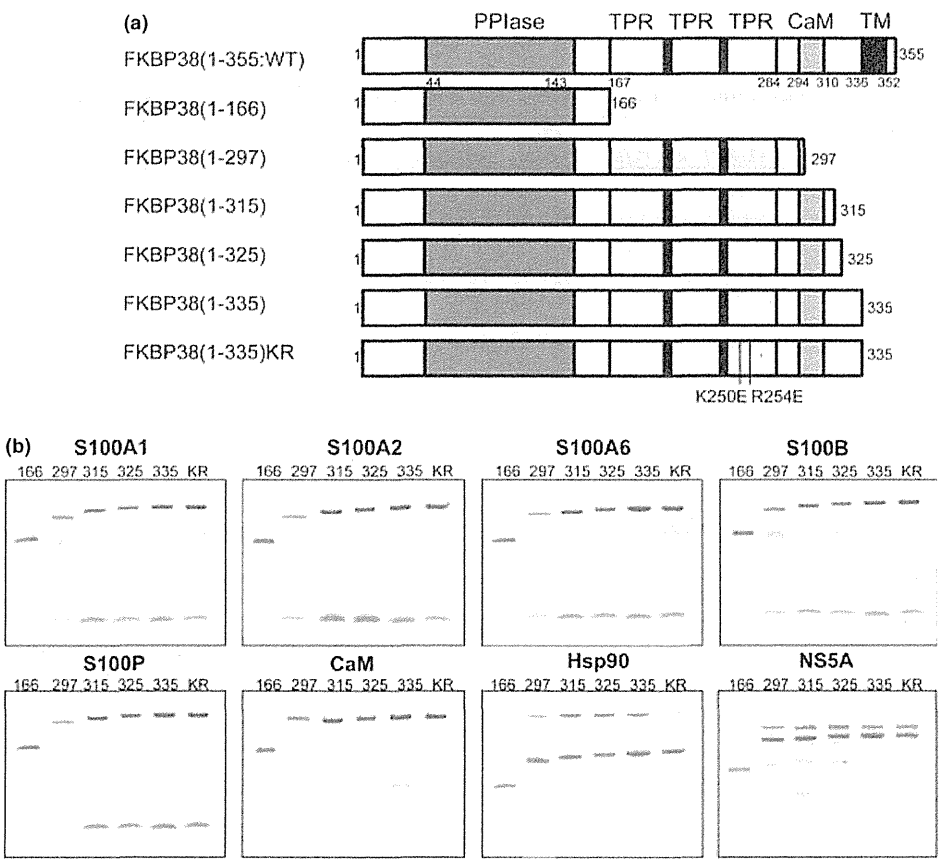

Fig. 3. Interaction of the FKBP8/FKBP38 mutants with the S100 proteins, Hsp90 and NS5A. (a) Schematic diagrams of the FKBP38 mutants. The number refers to the amino acid positions of FKBP38. The peptidyl prolyl *cis/trans* isomerases (PPIase), tetratricopeptide repeat (TPR), calmodulin-binding site (CaM) and transmembrane domain (TM) are shown. (b) The S-tag pull-down assay was performed using His_6-S-tag-FKBP38-WT and it's mutants. The His_6-S-tag-FKBP38 proteins (20 μg) and S100A1, S100A2, S100A6, S100B, S100P, CaM, Hsp90 or NS5A (25 μg each) were incubated with the S-protein agarose beads in the presence of 1 mM $CaCl_2$. Beads were washed and the eluted samples were analysed via a 10% Tricine–SDS-PAGE, followed by Coomassie Blue staining.

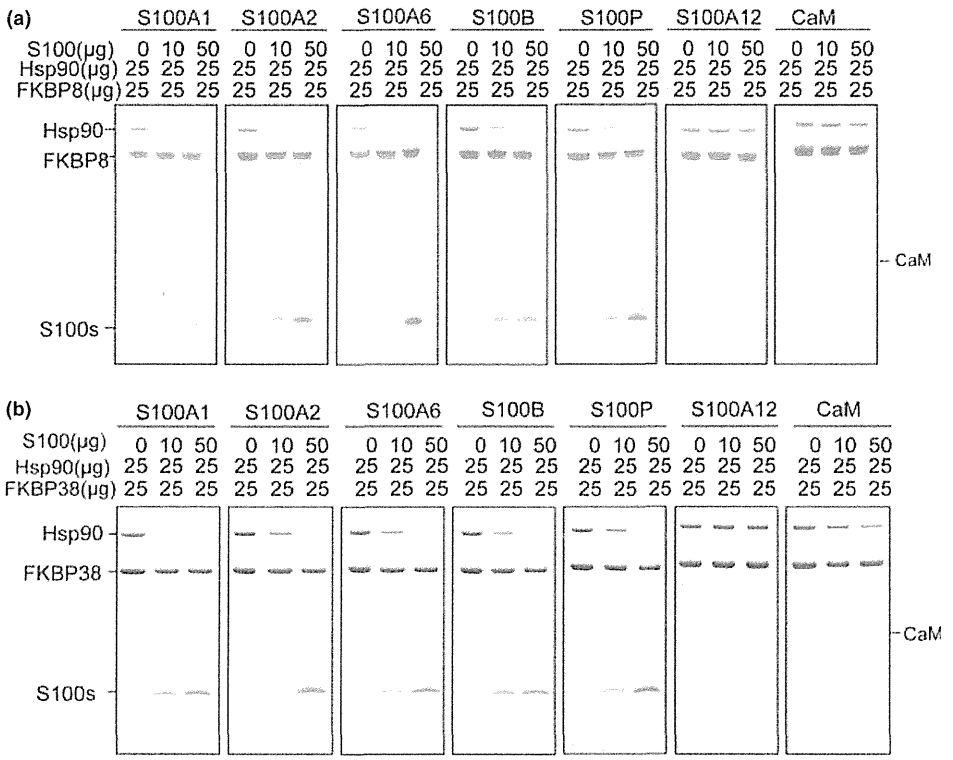

Fig. 4. S100 proteins competitively inhibit Hsp90 binding to FKBP8/FKBP38 *in vitro*. His_6-S-tag-FKBP8 (a, 25 μg) or His_6-S-tag-FKBP38 (b, 25 μg), Hsp90 (25 μg) and increasing amounts of the S100 proteins or CaM (0, 10 and 50 μg) were incubated with S-protein agarose beads in the presence of 1 mM $CaCl_2$ for 1 h. The S-tag pull-down assay was performed as described. Beads were washed and the eluted samples were analysed using a 10% Tricine–SDS-PAGE, followed by Coomassie Blue staining.

this further, a competitive binding assay was also performed with NS5A and His_6-S-tag-FKBP8/FKBP38 (Fig. 5). The addition of purified S100A1, S100A2, S100A6, S100B, S100P and CaM to the binding reactions substantially reduced the amount of NS5A retained on the immobilized His_6-S-tag-FKBP8 (Fig. 5a) and His_6-S-tag-FKBP38 (Fig. 5b). A significant competition was not observed with S100A12 (Figs 4 and 5).

S100 proteins have an inhibitory role in the replication of HCV RNA

The *in vitro* data described above suggest that Ca^{2+}/S100 proteins bind to the TPR domain of FKBP8/FKBP38, and lead to the inhibition of interactions of the FKBP8/FKBP38–Hsp90 and FKBP8/FKBP38–NS5A. Next, to examine whether these interactions are involved in HCV replication, the effect of the overexpression of the S100 protein in combination with ionophore treatment was studied in the HCV replicon harbouring cell line (sO cells) by measuring the amount of the NS3 protein (Fig. 6). We transfected the sO cells with S100A1 (Fig. 6a), S100A2 (Fig. 6b) and S100A6 (Fig. 6c). Following the transfection, the cells were treated with or without A23187 (5 μM) for 6, 12 and 24 h, and the cellular level of NS3 was examined via Western blot analysis using an anti-NS3 antibody. In the control replicon cells, the amount of NS3 did not change in the presence or absence of A23187 treatment. When the S100 proteins were overexpressed, the amount of NS3 was significantly decreased over the incubation period compared with the levels observed in the control cells (*lane 4* vs. *lane 2*). This suggested that increasing the concentration of intracellular Ca^{2+} stimulated the S100 proteins–FKBP8/FKBP38 complex formation, which inhibited the NS5A–FKBP8/FKBP38 and Hsp90–FKBP8/FKBP38 interactions and led to suppress the rate of NS3 production. Collectively, these results demonstrate that the S100 proteins may function as negative regulators of HCV replication in a Ca^{2+}-dependent manner.

Discussion

Hepatitis C virus replication occurs in the cytoplasm and is mediated by a membrane-associated replicase complex consisting of the NS3/NS4A, NS4B, NS5A and NS5B proteins and cellular proteins (host factors) (30).

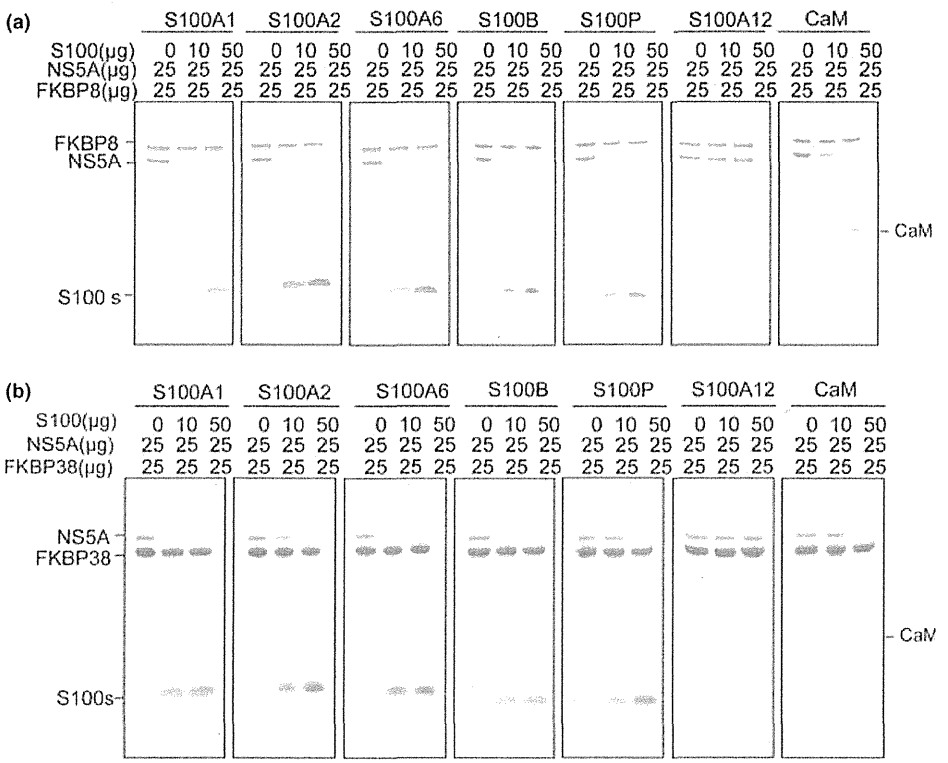

Fig. 5. S100 proteins competitively inhibit NS5A binding to FKBP8/FKBP38 *in vitro*. His_6-S-tag-FKBP8 (a, 25 μg) or His_6-S-tag-FKBP38 (b, 25 μg), NS5A (25 μg) and increasing amounts of the S100 proteins or CaM (0, 10 and 50 μg) were incubated with S-protein agarose beads in the presence of 1 mM $CaCl_2$. The S-tag pull-down assay was performed as described. Beads were washed and the eluted samples were analysed using a 10% Tricine–SDS-PAGE, followed by Coomassie Blue staining.

Importantly, the NS5A of HCV plays a critical role in HCV replication and is an attractive target for antiviral therapy of HCV infection (7).

NS5A is a multifunctional 56–58 kDa serine phosphoprotein and interacts with a number of cellular proteins thereby affecting numerous host functions, including the modulation of signal transduction pathways, suppression of apoptosis and modulation of transcription (8–10). Several cellular proteins, such as hVAP-A (31), hVAP-B (32), FKBP8 (11, 12), Hsp90 (11, 12), Hsp70 (33) and cyclophilin A, B (34, 35) are involved in the replication process of HCV. A recent report indicated that NS5A specifically interacts with FKBP8 via its TPR domain and recruits Hsp90 to the replicase complex; this complex formation is critical for the replication of HCV and thus geldanamycin was able to inhibit the RNA replication in a dose-dependent manner (11). *In vitro* pull-down assays revealed that geldanamycin inhibited the binding of FKBP8 to Hsp90 and/or NS5A domain I. In addition, the interaction between NS5A and FKBP38 disrupts FKBP38-mediated mTOR regulation (10). Moreover, NS5A inhibits apoptosis, potentially via the stabilization of the FKBP38–Hsp90 interactions (36).

TPR proteins are involved in many protein–protein interactions (14, 15); in particular, several cochaperones, including Hip, Hop and the cyclophilins, interact with Hsp70 or Hsp90 through TPR domains (37–40). The intracellular $Ca2^+$ signalling cascade is composed of many molecular components including a large family of EF-hand $Ca2^+$-binding proteins such as calmodulin (CaM), neuronal calcium sensor proteins and S100 proteins (41).

The S100 protein family is composed of at least 25 members that share two EF-hand motifs, a 25–65% amino acid sequence homology, and a molecular weight of 10–12 kDa (16–18).

S100 proteins are proposed to have intracellular and extracellular roles in the regulation of many cellular processes such as cell motility, cell-cycle progression, transcription, protein phosphorylation and tumour progression or suppression (16–18). Recently, we demonstrated that S100A2 and S100A6 interacted with the TPR domains of Hop, KLC and Tom70 in a Ca^{2+}-dependent manner, leading to the dissociation of the Hsp90-Hop-Hsp70, KLC-c-Jun N-terminal kinase-interacting protein-1 (JIP-1) and Tom70–Hsps interactions (19). Further studies revealed that the interaction

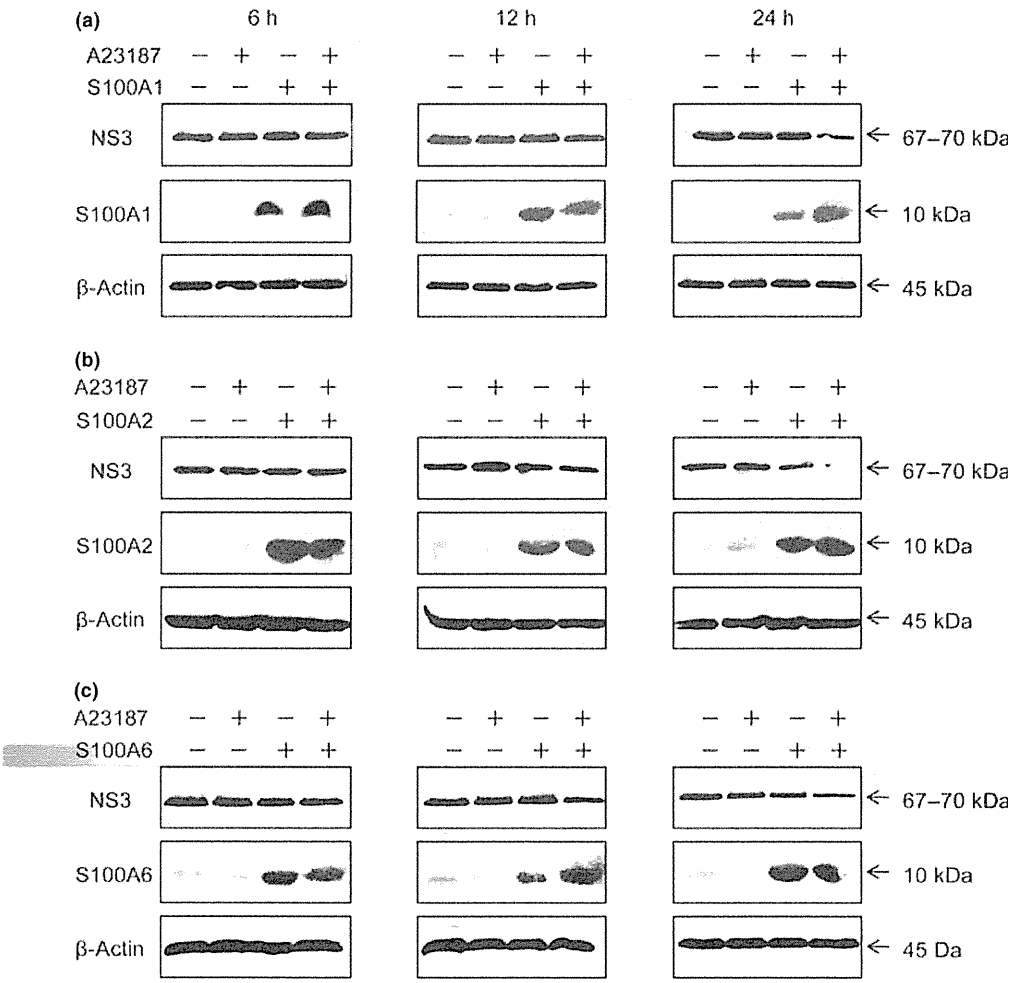

Fig. 6. S100 proteins suppress the cellular level of NS3 in HCV replicon harbouring cells (sO cells). HCV replicon harbouring cells (sO cells) were transiently transfected with (+) or without (−) S100A1 (a), S100A2 (b) and S100A6 (c) as indicated. After A23187 (5 μM) treatment, cell lysates were prepared at different time points (6, 12 and 24 h). The amount of NS3 and S100 proteins was analysed via Western blot analysis with the indicated antibodies. Equal amounts of lysates (20 μg of protein) were loaded in each lane for each time point. β-Actin was used as a control for equal loading.

of S100A1 and S100A2 with FKBP52 and Cyp40, which contain TPR domains, in the presence of Ca^{2+} led to the inhibition of the interactions of Cyp40–Hsp90 and FKBP52–Hsp90 (20).

In this study, we demonstrated that specific members of the S100 proteins, such as S100A1, S100A2, S100A6, S100B and S100P, specifically bind to the TPR domain of FKBP8/FKBP38 in a Ca^{2+}-dependent manner and lead to the inhibition of the Hsp90–FKBP8/FKBP38 interaction. The charged residues in the FKBP8/FKBP38-TPR domains are predicted to form the so-called two-carboxylate clamp form salt bridges with the EEVD of HSP90, and point mutations in the carboxylate clamp diminished the binding (11). Because S100 proteins interfered with the binding of Hsp90 to FKBP8/FKBP38, we anticipated that they bound to the amino acid residues composing the carboxylate clamp. However, S100 proteins bound to the alanine mutants of the carboxylate clamp, although Hsp90 binding was clearly inhibited (Fig. 3b). The results suggested that the mode of interaction of the S100 proteins with FKBP8/FKBP38 is different from the FKBP8/FKBP38–Hsp90 electrostatic interaction.

To explore further the interaction between FKBP8/FKBP38 and the S100 proteins, we investigated whether the S100 proteins inhibited the NS5A–FKBP8/FKBP38 interactions. Surprisingly, these S100 proteins effectively disrupted the NS5A–FKBP8/FKBP38 interactions. The binding site of S100 proteins may be close enough to physically interfere with the Hsp90 and NS5A binding to FKBP8/FKBP38. We have previously shown that the S100 proteins bind to TPR domains of Hop, KLC,

Tom70, Cyp40 and FKBP52, and result in the inhibition of the ligand–TPR protein interactions (19, 20). Notably, there is a preference in S100 protein binding among the TPR proteins. For example, S100A2 bound to KLC, FKBP52 and PP5 more tightly, whereas S100A6 preferably bound to Hop, Cyp40 and Tom70. The reason for the selectivity of S100 protein binding to TPR proteins is not fully understood. Currently, it is not possible to predict the residues that are important for the S100–TPR protein interactions.

Because the ternary complex formation of Hsp90, NS5A and FKBP8/FKBP38 is essential for the replication of HCV, it is important to determine whether the S100 proteins function as 'HCV-replication regulator' in intact cells. Using the HCV replicon harbouring cells (sO cells), the overexpression of S100A1, S100A2 and S100A6 in combination with ionomycin treatments showed a significant decrease in the protein level of NS3. The result suggests that the increase in intracellular Ca^{2+} by the treatment of ionomycin stimulated the binding of the S100 proteins and FKBP8/FKBP38, and inhibited the replication of HCV *in vivo*.

In conclusion, our results are the first to demonstrate that the association of the S100 proteins with FKBP8/FKBP38 provides a Ca^{2+}-dependent regulatory mechanism for the replication of HCV through the regulation of the formation of the NS5A–FKBP8/FKBP8–Hsp90 complex. These findings provide a new intracellular Ca^{2+}-signalling pathway via the interactions of the S100 protein–TPR motif.

Acknowledgements

We would like to thank Dr. Craig E Cameron (Pennsylvania State University) for kindly providing the HCV NS5A plasmids. This research is supported by the Kagawa University Characteristic Prior Research Fund for 2011 (to R.K.).

Disclosures

The authors disclose no competing interests

References

1. Lauer GM, Walker BD. Hepatitis C virus infection. *N Engl J Med* 2001; **345**: 41–52.
2. Thomson BJ, Finch RG. Hepatitis C virus infection. *Clin Microbiol Infect* 2005; **11**: 86–94.
3. Pawlotsky JM. Pathophysiology of hepatitis C virus infection and related liver disease. *Trends Microbiol* 2004; **12**: 96–102.
4. Shepard CW, Finelli L, Alter MJ. Global epidemiology of hepatitis C virus infection. *Lancet Infect Dis* 2005; **5**: 558–67.
5. Grakoui A, Wychowski C, Lin C, Feinstone SM, Rice CM. Expression and identification of hepatitis C virus polyprotein cleavage products. *J Virol* 1993; **67**: 1385–95.
6. Hijikata M, Kato N, Ootsuyama Y, Nakagawa M, Shimotohno K. Gene mapping of the putative structural region of the hepatitis C virus genome by in vitro processing analysis. *Proc Natl Acad Sci USA* 1991; **88**: 5547–51.
7. Macdonald A, Harris M. Hepatitis C virus NS5A: tales of a promiscuous protein. *J Gen Virol* 2004; **85**: 2485–502.
8. He Y, Nakao H, Tan SL, *et al.* Subversion of cell signaling pathways by hepatitis C virus nonstructural 5A protein via interaction with Grb2 and P85 phosphatidylinositol 3-kinase. *J Virol* 2002; **76**: 9207–17.
9. Street A, Macdonald A, Crowder K, Harris M. The hepatitis C virus NS5A protein activates a phosphoinositide 3-kinase-dependent survival signaling cascade. *J Biol Chem* 2004; **279**: 12232–41.
10. Peng L, Liang D, Tong W, Li J, Yuan Z. Hepatitis C virus NS5A activates the mammalian target of rapamycin (mTOR) pathway, contributing to cell survival by disrupting the interaction between FK506-binding protein 38 (FKBP38) and mTOR. *J Biol Chem* 2010; **285**: 20870–81.
11. Okamoto T, Nishimura Y, Ichimura T, *et al.* Hepatitis C virus RNA replication is regulated by FKBP8 and Hsp90. *EMBO J* 2006; **25**: 5015–25.
12. Okamoto T, Omori H, Kaname Y, *et al.* A single-amino-acid mutation in hepatitis C virus NS5A disrupting FKBP8 interaction impairs viral replication. *J Virol* 2008; **82**: 3480–9.
13. Hirano T, Kinoshita N, Morikawa K, Yanagida M. Snap helix with knob and hole: essential repeats in S. pombe nuclear protein nuc2+. *Cell* 1990; **60**: 319–28.
14. D'Andrea LD, Regan L. TPR proteins: the versatile helix. *Trends Biochem Sci* 2003; **28**: 655–62.
15. Allan RK, Ratajczak T. Versatile TPR domains accommodate different modes of target protein recognition and function. *Cell Stress Chaperones* 2011; **16**: 353–67.
16. Donato R. Functional roles of S100 proteins, calcium-binding proteins of the EF-hand type. *Biochim Biophys Acta* 1999; **1450**: 191–231.
17. Heizmann CW, Fritz G, Schafer BW. S100 proteins: structure, functions and pathology. *Front Biosci* 2002; **7**: d1356–68.
18. Donato R. S100: a multigenic family of calcium-modulated proteins of the EF-hand type with intracellular and extracellular functional roles. *Int J Biochem Cell Biol* 2001; **33**: 637–68.
19. Shimamoto S, Takata M, Tokuda M, *et al.* Interactions of S100A2 and S100A6 with the tetratricopeptide repeat proteins, Hsp90/Hsp70-organizing protein and kinesin light chain. *J Biol Chem* 2008; **283**: 28246–58.
20. Shimamoto S, Kubota Y, Tokumitsu H, Kobayashi R. S100 proteins regulate the interaction of Hsp90 with cyclophilin 40 and FKBP52 through their tetratricopeptide repeats. *FEBS Lett* 2010; **584**: 1119–25.
21. Ikeda M, Abe K, Dansako H, *et al.* Efficient replication of a full-length hepatitis C virus genome, strain O, in cell culture, and development of a luciferase reporter system. *Biochem Biophys Res Commun* 2005; **329**: 1350–9.
22. Kato N, Sugiyama K, Namba K, *et al.* Establishment of a hepatitis C virus subgenomic replicon derived from human hepatocytes infected in vitro. *Biochem Biophys Res Commun* 2003; **306**: 756–66.
23. Yurimoto S, Hatano N, Tsuchiya M, *et al.* Identification and characterization of wolframin, the product of the wolfram syndrome gene (WFS1), as a novel calmodulin-binding protein. *Biochemistry* 2009; **48**: 3946–55.

24. Tokumitsu H, Hatano N, Tsuchiya M, *et al.* Identification and characterization of PRG-1 as a neuronal calmodulin-binding protein. *Biochem J* 2010; **431**: 81–91.
25. Huang L, Sineva EV, Hargittai MR, *et al.* Purification and characterization of hepatitis C virus non-structural protein 5A expressed in escherichia coli. *Protein Expr Purif* 2004; **37**: 144–53.
26. Okada M, Hatakeyama T, Itoh H, *et al.* S100A1 is a novel molecular chaperone and a member of the Hsp70/Hsp90 multichaperone complex. *J Biol Chem* 2004; **279**: 4221–33.
27. Yamashita K, Oyama Y, Shishibori T, *et al.* Purification of bovine S100A12 from recombinant escherichia coli. *Protein Expr Purif* 1999; **16**: 47–52.
28. Hayashi N, Izumi Y, Titani K, Matsushima N. The binding of myristoylated N-terminal nonapeptide from neuro-specific protein CAP-23/NAP-22 to calmodulin does not induce the globular structure observed for the calmodulin-nonmyristylated peptide complex. *Protein Sci* 2000; **9**: 1905–13.
29. Scheufler C, Brinker A, Bourenkov G, *et al.* Structure of TPR domain-peptide complexes: critical elements in the assembly of the Hsp70-Hsp90 multichaperone machine. *Cell* 2000; **101**: 199–210.
30. Moriishi K, Matsuura Y. Host factors involved in the replication of hepatitis C virus. *Rev Med Virol* 2007; **17**: 343–54.
31. Tu H, Gao L, Shi ST, *et al.* Hepatitis C virus RNA polymerase and NS5A complex with a SNARE-like protein. *Virology* 1999; **263**: 30–41.
32. Hamamoto I, Nishimura Y, Okamoto T, *et al.* Human VAP-B is involved in hepatitis C virus replication through interaction with NS5A and NS5B. *J Virol* 2005; **79**: 13473–82.
33. Gonzalez O, Fontanes V, Raychaudhuri S, *et al.* The heat shock protein inhibitor quercetin attenuates hepatitis C virus production. *Hepatology* 2009; **50**: 1756–64.
34. Watashi K, Ishii N, Hijikata M, *et al.* Cyclophilin B is a functional regulator of hepatitis C virus RNA polymerase. *Mol Cell* 2005; **19**: 111–22.
35. Nakagawa M, Sakamoto N, Tanabe Y, *et al.* Suppression of hepatitis C virus replication by cyclosporin a is mediated by blockade of cyclophilins. *Gastroenterology* 2005; **129**: 1031–41.
36. Simonin Y, Disson O, Lerat H, *et al.* Calpain activation by hepatitis C virus proteins inhibits the extrinsic apoptotic signaling pathway. *Hepatology* 2009; **50**: 1370–9.
37. Blatch GL, Lassle M. The tetratricopeptide repeat: a structural motif mediating protein-protein interactions. *BioEssays* 1999; **21**: 932–9.
38. Nelson GM, Huffman H, Smith DF. Comparison of the carboxy-terminal DP-repeat region in the co-chaperones hop and hip. *Cell Stress Chaperones* 2003; **8**: 125–33.
39. Chen S, Smith DF. Hop as an adaptor in the heat shock protein 70 (Hsp70) and hsp90 chaperone machinery. *J Biol Chem* 1998; **273**: 35194–200.
40. Pratt WB, Toft DO. Regulation of signaling protein function and trafficking by the hsp90/hsp70-based chaperone machinery. *Exp Biol Med (Maywood)* 2003; **228**: 111–33.
41. Schafer BW, Heizmann CW. The S100 family of EF-hand calcium-binding proteins: functions and pathology. *Trends Biochem Sci* 1996; **21**: 134–40.

Cell Host & Microbe
Article

Antimicrobial Peptide LL-37 Produced by HSV-2-Infected Keratinocytes Enhances HIV Infection of Langerhans Cells

Youichi Ogawa,[1] Tatsuyoshi Kawamura,[1,*] Takamitsu Matsuzawa,[1] Rui Aoki,[1] Peter Gee,[4] Atsuya Yamashita,[2] Kohji Moriishi,[2] Kenshi Yamasaki,[3] Yoshio Koyanagi,[4] Andrew Blauvelt,[5] and Shinji Shimada[1]
[1]Department of Dermatology
[2]Department of Microbiology
Faculty of Medicine, University of Yamanashi, Yamanashi 409-3898, Japan
[3]Department of Dermatology, Tohoku University Graduate School of Medicine, Sendai 980-8575, Japan
[4]Laboratory of Viral Pathogenesis, Institute for Virus Research, Kyoto University, Kyoto 606-8507, Japan
[5]Oregon Medical Research Center, Portland, OR 97223, USA
*Correspondence: tkawa@yamanashi.ac.jp
http://dx.doi.org/10.1016/j.chom.2012.12.002

SUMMARY

Herpes simplex virus (HSV)-2 shedding is associated with increased risk for sexually acquiring HIV. Because Langerhans cells (LCs), the mucosal epithelium resident dendritic cells, are suspected to be one of the initial target cell types infected by HIV following sexual exposure, we examined whether and how HSV-2 affects HIV infection of LCs. Although relatively few HSV-2/HIV-coinfected LCs were detected, HSV-2 dramatically enhanced the HIV susceptibility of LCs within skin explants. HSV-2 stimulated epithelial cell production of antimicrobial peptides (AMPs), including human β defensins and LL-37. LL-37 strongly upregulated the expression of HIV receptors in monocyte-derived LCs (mLCs), thereby enhancing their HIV susceptibility. Culture supernatants of epithelial cells infected with HSV-2 enhanced HIV susceptibility in mLCs, and this effect was abrogated by blocking LL-37 production. These data suggest that HSV-2 enhances sexual transmission of HIV by increasing HIV susceptibility of LCs via epithelial cell production of LL-37.

INTRODUCTION

Epidemiologic studies have indicated a strong association between the acquisition of HIV and other sexually transmitted diseases (STDs) (Galvin and Cohen, 2004). This link is especially evident in cases of genital ulcer diseases (GUDs), with a 2- to 11-fold increase in the rate of HIV acquisition in the presence of GUD (Cameron et al., 1989; Fleming and Wasserheit, 1999). It is widely recognized that herpes simplex virus type 2 (HSV-2) is a major cause of GUDs, and more than 50 epidemiologic studies have now indicated that HSV-2 shedding is associated with increased risk for acquiring HIV (Wald and Link, 2002). The risk ratio of HIV acquisition for a person with genital herpes is enhanced from 2 to 4 when compared with a person without genital herpes, and potentially 50% of new HIV infections are considered to be attributable or worsened by HSV-2 infection (Wald and Link, 2002).

During sexual transmission of HIV, virus crosses mucosal epithelium and is eventually transmitted to regional lymph nodes, where it establishes permanent infection. Many studies have shown that Langerhans cells (LCs) are one of the important initial cellular targets for HIV, and that this particular type of dendritic cell (DC) plays a crucial role in disseminating HIV (de Witte et al., 2007; Kawamura et al., 2005; Lederman et al., 2006; Shattock and Moore, 2003). LCs are present within genital skin (e.g., outer foreskin) and mucosal epithelium and, after contact with pathogens, readily emigrate from tissue to draining lymph nodes. Immature resident LCs express surface CD4 and CCR5, but not surface CXCR4 (Zaitseva et al., 1997). These LCs are readily infected ex vivo with R5 HIV, but not with X4 HIV (Kawamura et al., 2000, 2008; Reece et al., 1998; Zaitseva et al., 1997). These findings are consistent with previous epidemiologic observations, which have found that the majority of HIV strains isolated from newly infected patients are R5 HIV strains (Zhu et al., 1993). It has been reported that persons with *CCR5* homozygous defects are largely protected from sexually acquiring HIV (Liu et al., 1996).

Clinical trials performed over the last several years have shown that circumcision greatly reduces the probability of penile HIV transmission, suggesting that the foreskin is an important portal of HIV entry (Auvert et al., 2005; Bailey et al., 2007; Gray et al., 2007). Although the mechanism leading to protection remains undefined, several ex vivo experiments with foreskin explants have indicated that CD4 T lymphocytes and LCs within foreskin epidermis are initial target cells for HIV (Fahrbach et al., 2010; Ganor et al., 2010; Grivel et al., 2011; Zhou et al., 2011).

In primate models of simian immunodeficiency virus (SIV) infection, there is controversy regarding which cells in the genital mucosa are initially infected by SIV. Studies have demonstrated that the primary infected cells present in the lamina propria of the cervicovaginal mucosa 48–72 hr after intravaginal exposure to SIV are T cells or submucosal DCs, but not epithelial LCs (Spira et al., 1996; Zhang et al., 1999). When vaginal tissue was examined within 1 hr following vaginal inoculation, however, up to

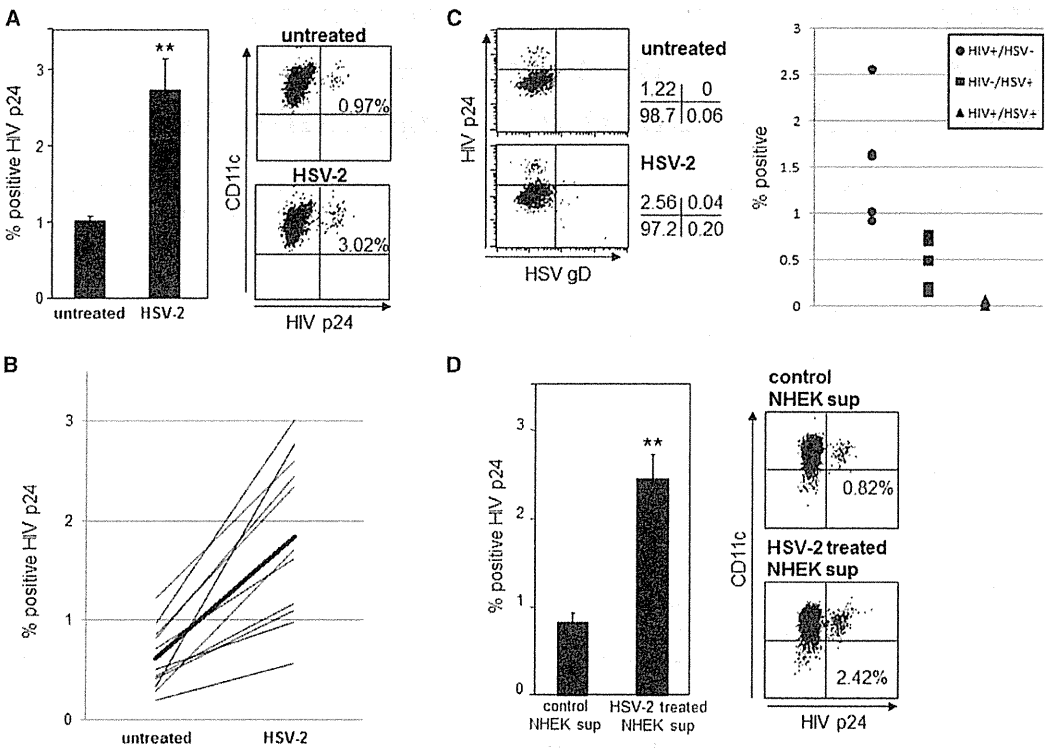

Figure 1. HSV-2-Infected Epithelial Cells Augment HIV Infection in LCs

(A–C) Epithelial sheets were preincubated with HSV-2 and then exposed to R5 HIV. Epithelial sheets were floated on culture medium to allow migration of LCs from the explants. Emigrating cells from the epidermal sheets were collected 3 days following HIV exposure. HIV-infected LCs were assessed by HIV p24 intracellular staining in langerin$^+$ CD11c$^+$ LCs (A) and the results of 11 separate experiments with different donors are summarized (B). HSV– and/or HIV-infected LCs were assessed by HIV p24 and HSV gD intracellular staining in CD11c$^+$ LCs, and the results from five different donors are summarized (C).

(D) mLCs were preincubated with the supernatants from NHEKs treated with or without HSV-2, and then exposed to R5 HIV. HIV p24$^+$ cells were assessed in langerin$^+$ CD11c$^+$ mLCs at day 7.

(A, C, and D) Representative flow cytometric analyses are shown. (A and D) Results are shown as means ± SD (n = 3) (**$p < 0.01$). See also Figure S1.

90% of SIV-infected cells were found to be LCs (Hu et al., 2000). Because only a single layer of columnar epithelium guards the endocervix and the transformation zone, the mucosal barrier can be easily breached by mechanisms such as the microtrauma associated with sexual intercourse, which provides immediate access to target cells, especially CD4$^+$ T cells, in the submucosa (Haase, 2010). Indeed, it has been shown that following mucosal exposure to high doses of SIV, virus can gain access through breaks in the mucosal epithelial barrier and infect resting CD4$^+$ T cells in the submucosa (Haase, 2010). Since molecules targeting CCR5 completely protected against mucosal transmission of SHIV (Lederman et al., 2004), CD4/CCR5-mediated de novo infection of LCs and/or CD4$^+$ T cells is considered to be a major pathway involved in sexual transmission of HIV.

Several mechanisms have been proposed to explain enhanced sexual transmission of HIV during active STD infection, including breakdown of epithelial barriers (i.e., ulceration) with direct inoculation of HIV into the blood (Cunningham et al., 1985), presence of inflammatory leukocytes that act as targets (Zhu et al., 2009), and coinfection of cells by HIV and STD pathogens. Biological mechanisms responsible for greater HIV transmission rates in the presence of genital herpes infections, however, are as of yet unknown. Recently, we and others have suggested that HIV susceptibility of LCs could be directly enhanced by pathogens and indirectly enhanced by inflammatory factors during STD, thereby leading to more likely sexual transmission of HIV (de Jong et al., 2008; Ogawa et al., 2009). In this report, we found that HSV-2 primarily infected epithelial cells and then markedly enhanced HIV infection in adjacent LCs. Interestingly, mechanistic studies revealed that LL-37 produced by HSV-2-infected epithelial cells upregulated CD4 and CCR5 on the surface of bystander LCs, thereby enhancing HIV infection in these cells. These findings may lead to new strategies designed to block sexual transmission of HIV.

RESULTS

HSV-2 Indirectly Enhances HIV Susceptibility in LCs via Interaction with Epithelial Cells

We first examined whether HSV-2 modulates HIV susceptibility of LCs by using an ex vivo skin explant model, whereby resident LCs within epithelial tissue are exposed to HIV and then allowed to emigrate from tissue, thus mimicking conditions that occur following mucosal exposure to HIV (Kawamura et al., 2000).

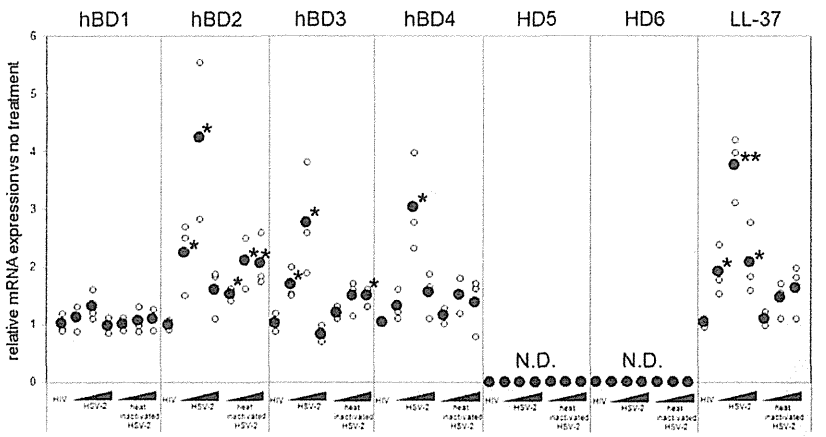

Figure 2. HSV-2 Increases Expression of Human β Defensin-2, Defensin-3, Defensin-4, and LL-37 in Normal Human Epithelial Cells

HIV-1 (10^5 $TCID_{50}$), HSV-2 ($1 \times 10^4 - 1 \times 10^6$ PFU), and heat-inactivated HSV-2 ($1 \times 10^4 - 1 \times 10^6$ PFU) were exposed to NHEKs for 1 hr and then washed twice. Cells were incubated in culture medium for 12 hr, and the mRNA expression of indicated AMPs was determined by qPCR. Results are shown as mean relative mRNA expressions (○) from three different experiments and mean the average (●) of those (*$p < 0.05$; **$p < 0.01$). See also Figure S2.

Epidermal sheets obtained from suction blister roofs were exposed to HSV-2 strain G at 1×10^6 PFU/tissue for 1 hr, and then exposed to R5-tropic HIV-1_{BaL} for 2 hr. Three days later, to quantify numbers of HIV-infected LCs at the single-cell level, cells emigrating from the explants were stained with anti-CD11c, anti-langerin, and anti-HIV p24 mAbs. Intracellular staining for HIV p24 represents productive HIV replication within LCs, since expression can be completely blocked by AZT (Kawamura et al., 2003). The numbers of LCs emigrating from individual explants were determined, and the mean yield ± SD was HSV−/HIV−; $1.04 \pm 0.25 \times 10^4$, HSV−/HIV+; $1.13 \pm 0.31 \times 10^4$, HSV+/HIV−; $1.25 \pm 0.27 \times 10^4$; and HSV+/HIV+; $1.21 \pm 0.25 \times 10^4$ (n = 3). Thus, the number of LCs recovered from the skin explants was not significantly affected by HSV-2 or HIV exposure. However, preincubation of epithelial sheets with HSV-2 significantly increased the percentage of HIV $p24^+$ cells within $langerin^+$ $CD11c^+$ LCs approximately 3-fold as compared to LCs emigrating from nonexposed epithelial sheets (Figure 1A). The results of 11 separate experiments with different skin donors are summarized in Figure 1 B (mean percentage HIV $p24^+$ LCs ± SD = 0.61 ± 0.31 with no HSV-2; 1.85 ± 0.79 with HSV-2 preincubation, p = 0.0002, n = 11). To assess the ratio of individual HSV-2- and/or HIV-infected LCs emigrating from explants, cells were collected from cultures and stained with anti-CD11c, anti-HSV gD, and anti-HIV p24 mAbs. A recent study in mice showed that HSV impeded emigration of infected LCs by inducing apoptosis and by blocking E-cadherin downregulation (Miller et al., 2011b). Consistent with this finding, the percentage of HSV-2-infected emigrating LCs was much less when compared with LCs that remained within explants at day 3 (Figure 1C and see Figure S1 online). More importantly, we found that HSV-2/HIV-coinfected emigrating LCs were rarely detected (mean percentage of HIV-1 $p24^+$/HSV-2 gD^+ LCs ± SD = 0.04 ± 0.02, n = 5, Figure 1C), suggesting that HSV may not directly modulate HIV susceptibility in LCs. Indeed, supernatants from epithelial cell cultures of normal human epidermal keratinocytes (NHEKs) treated with HSV-2 also increased the percentage of HIV p24+ monocyte-derived LCs (mLCs), even though mLCs were not exposed to HSV-2 (Figure 1D). Of note, the magnitude of HIV susceptibility in mLCs enhanced by HSV-treated NHEK supernatants was comparable to that in emigrating LCs in the epithelial explant experiments. Enhancement of HIV infection by supernatants from HSV-2-treated NHEKs was dependent on the dose of HSV-2, and supernatants from heat-inactivated HSV-2-treated NHEKs did not affect HIV susceptibility in mLCs (Figure S2). HIV susceptibility in mLCs was also enhanced when we infected NHEKs with a second HSV-2 strain, 186 (data not shown). Taken together, these results suggest that HSV-2 indirectly mediates HIV infection of epidermal LCs by a soluble factor or factors released by HSV-2-infected epithelial cells.

HSV-2 Augments the Production of Antimicrobial Peptides from Keratinocytes, and LL-37 Enhances HIV Infection in LCs

In STDs, antimicrobial peptides (AMPs), including defensins and cathelicidin, are the key effector molecules of mucosal innate and adaptive immunity. Human vaginal epithelial cells and epidermal keratinocytes can produce human α defensin-5 (HD5), HD6 and human β defensin-1 (hBD1), hBD2, hBD3, hBD4, and the sole cathelicidin in humans, LL-37. Certain defensins (e.g., hBD1) are expressed constitutively, and others (e.g., hBD2 and hBD3) show increased expression in response to inflammation or infection (Klotman and Chang, 2006). Several reports have indicated that several of these AMPs modulate HIV infectivity in peripheral blood mononuclear cells (PBMC) or in $CD4^+$ T cells (Bergman et al., 2007; Klotman et al., 2008; Quiñones-Mateu et al., 2003; Sun et al., 2005). Thus, we investigated whether HSV-2 induced AMPs production in keratinocytes. NHEKs were incubated with HSV-2 ($1 \times 10^4 - 1 \times 10^6$ PFU) or HIV-1 (1×10^5 $TCID_{50}$), and relative mRNA expression levels of AMPs were determined by quantitative RT-PCR. Interestingly, HSV-2 significantly increased the expression of hBD2, hBD3, hBD4, and LL-37, whereas neither HIV nor heat-inactivated HSV-2 affected expression of hBD3, hBD4, and LL-37 (Figure 2).

To determine whether keratinocyte-derived AMPs affect HIV susceptibility of LCs, mLCs were stimulated with AMPs or TNF-α, as a positive control, for 24 hr before exposure to HIV-1. Strikingly, only LL-37 significantly increased the percentage of HIV $p24^+$ mLCs (Figure 3A). This infection-enhancing effect of LL-37 was observed in a dose-dependent manner, utilizing concentrations of LL-37 observed in physiologic conditions (Ong et al., 2002; Yamasaki et al., 2007) (Figure 3B). Interestingly, LL-37 also significantly upregulated surface expression

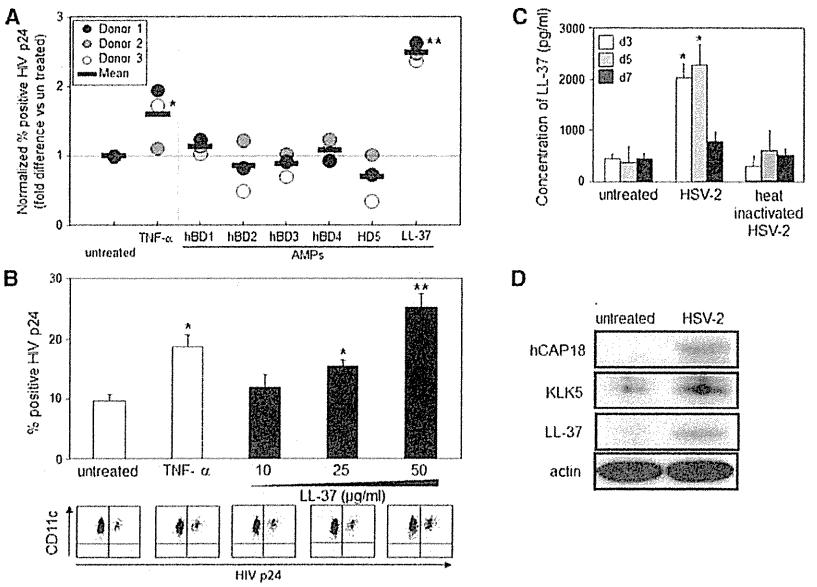

Figure 3. LL-37 Enhances HIV Susceptibility in mLCs

mLCs were stimulated with the indicated AMPs or rhTNF-α 24 hr prior to HIV exposure. To assess HIV infection levels, mLCs were collected 7 days after HIV exposure, and HIV p24$^+$ cells were quantified in langerin$^+$ CD11c$^+$ mLCs.

(A) Each circle indicates the normalized percentage of positive cells for HIV p24; mean values obtained from different donors are shown as horizontal marks.

(B) The percentage of positive cells for HIV p24 in langerin$^+$ CD11c$^+$ mLCs and representative flow cytometric analyses following LL-37 stimulation.

(C) NHEKs were exposed to HSV-2 or heat-inactivated HSV-2. Following culture for the indicated number of days, LL-37 levels were measured in supernatants by ELISA. Results are shown as means ± SD (n = 3) (*$p < 0.05$).

(D) NHEKs were treated with HSV-2 for 3 days and then lysed. The expression of hCAP18, KLK5, and LL-37 was determined by western blot analysis. All data shown represent at least two separate experiments. See also Figure S3.

of CD86, CD83, and CCR7 on mLCs (Figure S3), indicating that LL-37 induces LC maturation.

To confirm whether HSV-2-treated NHEKs could produce LL-37 protein, we measured LL-37 protein levels in culture supernatants from NHEKs treated with medium alone, HSV-2, or heat-inactivated HSV-2 by ELISA. HSV-2 significantly induced production of LL-37 in NHEKs, which peaked at day 5 (Figure 3C). Expression levels of kallikrein 5 (KLK5) have been shown to parallel induction of LL-37 in KCs, since the activity of cathelicidin is controlled by enzymatic processing of the proform hCAP18 to a mature peptide LL-37 by KLK5, a serine protease (Morizane et al., 2010; Yamasaki et al., 2006). Therefore, we measured protein levels of LL-37, hCAP18, and KLK5 in NHEKs treated with medium alone or HSV-2. As shown in Figure 3D, HSV-2 induced production of LL-37 in NHEKs. Similarly, HSV-2 increased expression of hCAP18 as well as KLK5, and these protein levels coincided with the induction of LL-37 in NHEKs (Figure 3D).

To further confirm the participation of LL-37 in this enhancement, we used RNA interference (siRNA) to block LL-37 production. Protein levels were quantified by western blotting followed by densitometry analysis. Transfection of siRNA targeting LL-37 induced an efficient knockdown in NHEKs (55% downregulation; Figure 4A). In line with the results of western blot analyses, siRNA-mediated interference of LL-37 in NHEKs significantly reduced enhancement of HIV infection in mLCs by supernatants from HSV-2-treated NHEKs, in comparison with control siRNA targeting an irrelevant sequence (Figure 4B). Based on these results, we conclude that enhanced HIV infection in mLCs by supernatants from HSV-2-treated NHEKs is, at least in part, mediated by LL-37.

Recently, TNF-α derived from KCs has also been shown to enhance HIV susceptibility of LCs (de Jong et al., 2008; Ogawa et al., 2009). In our experiments, however, TNF-α was not detected in culture supernatants from NHEKs treated by HSV-2 (data not shown), consistent with a recent report (de Jong et al., 2010). In addition, preincubation of supernatants from HSV-2-treated NHEKs with an anti-TNF-α neutralizing mAb, prior to exposing mLCs, did not affect HIV susceptibility in mLCs (Figure S4).

LL-37 Enhances Surface Expression of CD4 and CCR5 on mLCs

Previous studies have revealed that langerin expressed on LCs is a natural barrier to HIV infection because HIV virions captured by langerin are internalized into LC Birbeck granules and degraded (de Witte et al., 2007). In addition, APOBEC3G (A3G) and SAM domain and HD domain 1 (SAMHD1) has been recently shown to function as a potent postentry cellular restriction factor for HIV in DCs or LCs (Hrecka et al., 2011; Laguette et al., 2011; Ogawa et al., 2009; Pion et al., 2006). Therefore, we next examined whether LL-37 affects the expression levels of these molecules in mLCs. LL-37 stimulation did not affect the expression of langerin, A3G, or SAMHD1 (Figures 4C and 4D and Figure S5). In contrast, LL-37 significantly increased surface expression of CD4 and CCR5 on mLCs (Figure 4C). In addition, siRNA-mediated interference of LL-37 in NHEKs significantly reduced the enhancement of surface expression of CD4 and CCR5 in mLCs by supernatants from HSV-2-treated NHEKs, in comparison with control siRNA targeting an irrelevant sequence (Figure 4C). Thus, our results suggest that LL-37 enhances HIV infection in LCs by increasing surface expression of HIV receptors, rather than by modulating restriction factors such as langerin, A3G, or SAMHD1.

Since LL-37 upregulated surface expression of CD4 and CCR5 in LCs, we next examined whether LL-37 specifically enhanced R5-tropic HIV entry into LCs by using single-round infection assays with pseudotyped viruses containing a luciferase reporter and different envelope proteins (Env): Env from either R5 HIV-1 (JR-FL; R5), X4 HIV-1 (IIIB; X4), or vesicular stomatitis virus (VSV-G). As expected, we found that LL-37 pretreatment enhanced the infectivity of mLCs to R5-VSV in

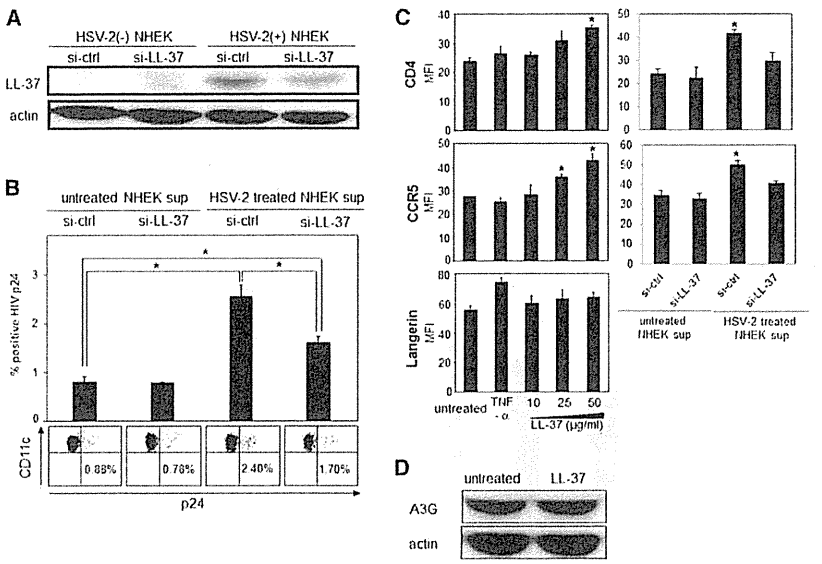

Figure 4. Silencing of LL-37 in HSV-2-Infected NHEKs Abrogates Enhanced HIV Infectivity in mLCs

(A) NHEKs were transfected with control or LL-37 siRNA and then exposed with or without HSV-2. Cells were lysed and then determined the expression of LL-37 by western blot analysis.

(B) mLCs were incubated with indicated culture supernatants for 12 hr and then exposed to R5 HIV. mLCs were collected 7 days after the HIV exposure, and HIV p24$^+$ cells were assessed in langerin$^+$ CD11c$^+$ mLCs. Representative flow cytometric analyses of CD11c and p24 mAb double-stained cells are shown.

(C) mLCs were stimulated with TNF-α or LL-37 at the indicated concentrations or indicated culture supernatants for 24 hr. The expression of CD4, CCR5, and langerin was assessed by flow cytometry.

(D) The expression of A3G was determined by western blot analysis. Results are shown as means ± SD (n = 3) (*$p < 0.05$). All data shown represent at least two separate experiments. See also Figure S4.

a dose-dependent manner, but LL-37 did not affect infection with VSV-G (Figure 5A). Consistent with previous findings (Kawamura et al., 2001), mLCs were resistant to X4-VSV, even after LL-37 treatment. These results provide direct evidence that LL-37, which upregulates surface expression of CD4 and CCR5 in LCs, promotes increased R5 HIV entry into these cells. Furthermore, similar effects of LL-37 were observed when mLCs were infected with R5 HIV primary isolates: JR-FL and AD8 (Figures 5B and 5C).

LL-37 Decreases HIV Infectivity in mDCs

We next examined whether LL-37 affects HIV infectivity in non-LC-like DCs. Similar to mLCs, LL-37 significantly upregulated surface expression of CD86 and CCR7 on monocyte-derived DCs (mDCs, Figure S3), indicating that LL-37 induces DC maturation. In marked contrast to mLCs, however, there was inhibition of HIV infection in mDCs when these cells were preincubated with LL-37 prior to HIV exposure (Figure 6A), indicating that LL-37 effects on HIV infectivity are differentially regulated in LCs and DCs. LL-37 did not affect CD4 or A3G expression in DCs but markedly downregulated surface expression of CCR5 and DC-SIGN (Figures 6B and 6C). It has been shown that DC-SIGN binds HIV and plays a critical role for HIV replication in mDCs (Gringhuis et al., 2010). These results, in contrast to mLCs, suggest that decreased HIV infection levels observed in LL-37-treated mDCs may be due to downregulation of DC-SIGN and/or CCR5 on their cell surfaces. Taken together, our results indicated the presence of exclusive machinery to augment HIV infection by LL-37 in LC in contrast to that in CD4$^+$ T cells (Bergman et al., 2007) and mDCs.

LL-37 Enhances HIV Transmission from LCs to CD4$^+$ T Cells

We next examined whether LL-37 affected HIV transmission from LCs to cocultured CD4$^+$ T cells. mLCs or mDCs were stimulated with AMPs or TNF-α for 24 hr, exposed to HIV-1_{Ba-L}, and then cocultured with allogeneic CD4$^+$ T cells for 12 days. Consistent with results showing that LL-37 increases HIV infection levels in mLCs (Figure 3A), preincubation of mLCs with LL-37 significantly enhanced subsequent HIV transmission from mLCs to CD4$^+$ T cells in a dose-dependent manner; preincubation with other AMPs did not affect HIV transmission levels in mLC-T cell cocultures (Figure 7A). By contrast, HIV transmission from mDCs to CD4$^+$ T cells was significantly decreased by preincubation of mDCs with LL-37 (Figure 7B), consistent with decreased HIV infection levels in LL-37-treated mDCs (Figure 6A).

DISCUSSION

LCs are generally believed to be one of the cell types that plays a pivotal role in the dissemination of virus during sexual transmission of HIV. To understand the biologic mechanisms by which HSV-2 increases acquisition of HIV, we tested the hypothesis that HSV-2 modulates LC susceptibility to HIV. As expected, we found that HSV-2 enhances HIV susceptibility of LCs within epithelial tissue (Figure 1), consistent with a recent finding that HSV-2 directly enhances HIV susceptibility in LCs (de Jong et al., 2010). However, in our ex vivo explant model, the percentage of HSV/HIV-coinfected LCs was quite low. Instead, our findings suggested that HSV-2 increases HIV susceptibility in LCs by indirect (i.e., epithelial cell-dependent) mechanisms. More specifically, we show here that LL-37 produced by HSV-2-infected epithelial cells enhances HIV infection of LC, most likely by increasing surface expression of CD4 and CCR5 on these cells.

There are conflicting prior reports on how defensins affect HIV infectivity. A variety of anti-HIV activities for hBD2 and hBD3 have been reported, including direct inhibition of virions, indirect inhibition of HIV replication, and downregulation of HIV coreceptors (Klotman and Chang, 2006; Quiñones-Mateu et al., 2003). By contrast, other studies have shown increased HIV infection of

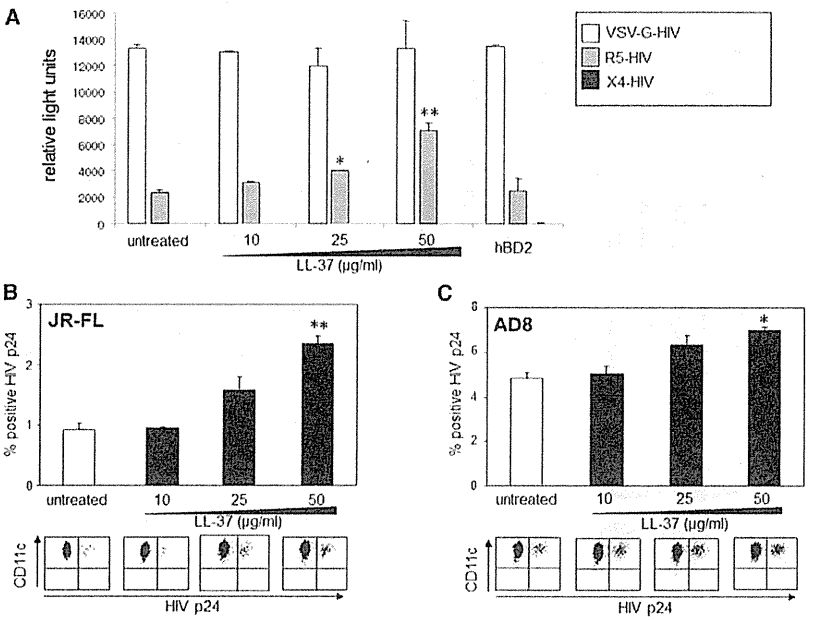

Figure 5. LL-37 Enhances mLCs Susceptibility to R5-HIV and R5 HIV Primary Isolates

mLCs were stimulated with LL-37 at the indicated concentration or hBD2 as control, and then exposed to pseudotyped viruses (R5-HIV, X4-HIV or VSV-G-HIV) for 72 hr (A) or R5 HIV primary isolates (JR-FL or AD8) for 2 hr (B and C). To assess pseudotyped virus infection levels, the average luciferase activity was calculated as relative light units (A). To assess primary HIV infection levels, mLCs were collected 7 days after the HIV exposure, and HIV p24$^+$ cells were assessed in langerin$^+$ CD11c$^+$ mLCs (upper panels, % of positive cells for HIV p24 in langerin$^+$ CD11c$^+$ mLCs; and lower panels, representative flow cytometric analyses following LL-37 stimulation). Results are shown as means ± SD (*$p < 0.05$; **$p < 0.01$). All data shown represent at least two separate experiments. See also Figure S5.

primary CD4$^+$ T cells by HD5 and HD6, and no effects on cell-surface HIV coreceptor expression by hBD1 and hBD2 (Klotman et al., 2008; Sun et al., 2005). These conflicting reports might be due to differences in experimental conditions or cell types used (e.g., PBMC or CD4$^+$ T cells). Interestingly, we found that, unlike PBMC and CD4$^+$ T cells, human β defensins did not affect HIV infectivity of LCs (Figure 3). Although no significant differences were detected, hBD2 and HD5 tended to decrease HIV infectivity of LCs. In addition, consistent with a previous finding that LL-37 inhibits HIV replication in CD4$^+$ T cells (Bergman et al., 2007), we found that LL-37 significantly inhibited HIV infectivity in DCs, probably through downregulation of surface DC-SIGN expression (Figure 6). By contrast, LL-37 upregulated surface expression of CD4 and CCR5 in LCs, and upregulation strongly correlated with the increased R5 HIV entry and infection within these cells (Figure 4 and Figure 5). Thus, these findings clearly indicate that the effects of AMPs on HIV infectivity are differentially regulated depending on the target cell type.

We found that HSV-2 infection in epithelial cells induced the production of soluble LL-37 that had potent enhancing effects on HIV infectivity in LCs. siRNA-mediated interference of LL-37 transcription blocked, at least in part, increased HIV infectivity. We hypothesize that when HSV-2 infection occurs in genital mucosa, LL-37 produced by HSV-infected epithelial cells augments HIV susceptibility of LCs, thereby leading to enhanced sexual transmission of HIV. Notably, a recent study has shown that cervicovaginal levels of LL-37 were associated with increased HIV acquisition in Kenyan sex workers (Levinson et al., 2009), a clinical finding that supports our hypothesis. Thus, HSV-2 can mediate both direct enhancing effects on HIV susceptibility in LCs as well as indirect enhancing effects via LL-37 production as shown here. These results further our understanding of the complex biologic events that occur during the early stages of sexual transmission of HIV.

EXPERIMENTAL PROCEDURES

Reagents

Cells were stimulated with synthetic AMPs (Peptide Institute) for 24 hr at the following concentrations: α defensin-5 (50 μg/ml), β defensin-1 (50 μg/ml), β defensin-2 (50 μg/ml), β defensin-3 (5 μg/ml), β defensin-4 (50 μg/ml), and LL-37 (50 μg/ml). Recombinant human (rh) TNF-α (5 μg/ml, R&D Systems) was used as a positive control in some experiments. Anti-TNF-α neutralizing mAbs (clone; MABTNF-A5) were purchased from BD PharMingen and used at a final concentration of 1 μg/ml.

Cell Preparation

NHEKs were purchased from Kurabo and cultured with EpiLife supplemented with insulin (10 μg/ml), rhEGF (epidermal growth factor, 0.1 ng/ml), hydrocortisone (0.5 μg/ml), gentamicin (50 μg/ml), amphotericin B (50 ng/ml), and bovine pituitary extract (0.4% V/V) (EpiLife-KG2 medium, all from Kurabo) in a humidified atmosphere with 5% CO2 at 37°C.

mLCs and mDCs were cultured from adult plastic-adherent PBMCs as described previously (Kawamura et al., 2001). Briefly, monocytes were isolated by depletion of magnetically labeled nonmonocytes (Monocyte Isolation Kit II, Miltenyi Biotec) from plastic-adherent PBMCs obtained from healthy blood donors. Monocytes were cultured in RPMI 1640 (GIBCO BRL) supplemented with 10% heat-inactivated FBS (Cell Culture Technologies), 100 U/ml penicillin (GIBCO BRL), 100 μg/ml streptomycin (GIBCO BRL), 2 mM L-glutamine (GIBCO BRL) (complete medium) supplemented with 1,000 U/ml rhGM-CSF (R&D Systems), 1,000 U/ml rhIL-4 (R&D Systems), and with mLCs or without mDCs 10 ng/ml human platelet-derived TGF-β1 (R&D Systems) for 7 days. Since we have previously found the expression levels of E-cadherin$^+$ cells and langerin$^+$ cells in mLCs to be approximately 90% and 35%, respectively (Kawamura et al., 2001), cell sorting was performed at day 7 to isolate highly purified langerin-positive mLCs followed by staining with anti-langerin mAb (Immunotech), as previously described (Ogawa et al., 2009). Alternatively, mLCs were identified by gating langerin-positive cells in flow cytometric analyses.

HSV-2 Exposure of Cells In Vitro and Skin Explants Ex Vivo

Purified, pelleted, and titered HSV-2 G strain (stock at 10^8 PFU/ml) was purchased from Advanced Biotechnologies. HSV-2 strain 186 (stock at 1.5×10^7 PFU/ml) was a gift from Yukihiro Nishiyama (Nagoya University Graduate School of Medicine, Nagoya, Japan). A total of 2×10^5 mLCs or mDCs, or 5×10^6 NHEK, were cultured with different concentrations of HSV-2 (10^{4-6} PFU) at 37°C, and then washed three times. In some experiments using the supernatants from NHEKs treated by HSV-2, culture supernatants

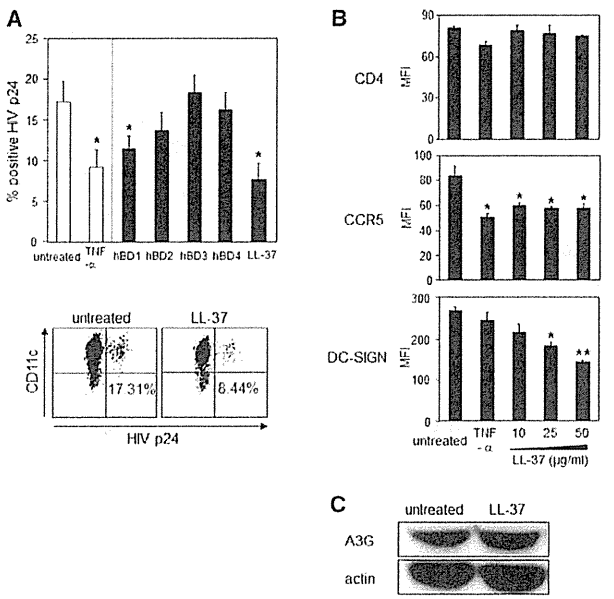

Figure 6. LL-37 Decreases HIV Susceptibility in mDCs

(A) mDCs were stimulated with the indicated AMPs or rhTNF-α 24 hr prior to HIV exposure. To determine HIV infection levels, mDCs were collected 7 days after HIV exposure, and HIV p24$^+$ cells were assessed in CD11c$^+$ mDCs. Representative flow cytometric analyses are shown.

(B) mDCs were stimulated with TNF-α or LL-37 at the indicated concentrations for 24 hr. The expression of CD4, CCR5, and DC-SIGN was assessed by flow cytometry.

(C) The expression of A3G was determined by western blot analysis. Results are shown as means ± SD (n = 3) (*p < 0.05; **p < 0.01). All data shown represent at least two separate experiments.

containing HSV-2 were filtered by PALL Acrodisc 32 mm Syringe Filter with 0.1 μm Supor Membrane to remove viruses. For control infection, the same batch of virus was inactivated at 56°C for 10 min and the same volume as the active virus was added to cells. For exposure of epithelial tissue explants, 50 μl droplets containing different concentrations of HSV-2 were placed on the inside surfaces of sterile plastic culture dish covers. Explants were draped over droplets with the basal epithelial cell surface facing downward. Virus and explants were incubated together in this manner at 37°C in a humidified 5% CO_2 environment for 1 hr, and then washed three times with cold PBS.

HIV Infection of Cells In Vitro and Skin Explants Ex Vivo

Purified, pelleted, and titered HIV-1Ba-L, an R5 HIV laboratory isolate (stock at $TCID_{50}$ of $10^{7.17}$/ml and 1.8 × 10^{10} virus particles/ml), was purchased from Advanced Biotechnologies. Molecular clones R5 HIV primary isolates (JR-FL and AD8) were prepared as described previously (Koyanagi et al., 1997; Theodore et al., 1996). Briefly, 293T cells were transfected with 30 μg of HIV-1 proviral DNA. One day after transfection, the medium was replaced with fresh RPMI 1640 medium supplemented with 10% FCS, and then 2 days later, the viruses were recovered, filtered through a membrane (pore size, 0.22 mm), and assayed for HIV-1 p24 gag content by ELISA. The titer of each virus stock was determined by endpoint titer determination of 3-fold limiting dilution in triplicate on PHA-activated PBMC from a single donor. Aliquots of the viral stocks ($TCID_{50}$ of 9,004,929/ml; JR-FL and 7,746,147/ml; AD8) were stored at minus 80°C until use. For some experiments, 2 × 10^5 mLCs and mDCs were preincubated with various agonists, inhibitors, HSV-2, or the supernatants from NHEKs treated by HSV-2, and then HIV-1Ba-L at a 1/100 final dilution or R5 HIV primary isolates (JR-FL and AD8) at $TCID_{50}$ of 10^5/ml was added for 2 hr at 37°C, as described previously (Kawamura et al., 2001). After incubation, cells were harvested, washed three times in washing medium (HBSS containing 10% heat-inactivated FBS), resuspended in complete medium supplemented with GM-CSF and IL-4, and cultured for 7 additional days at the same cellular concentration. HIV-infected cells were assessed by HIV p24 intracellular staining. Because the variability in the infection levels was most likely due to the *CCR5* heterogeneity in the donors, HIV infection levels with mLCs and mDCs obtained from different donors were not directly compared. Instead, HIV infection levels were expressed as a normalized percent of the positive cells for HIV p24 by using a calculated fold difference as compared with the mean percent of the positive cells for HIV p24 in untreated cells (Figure 3A). In some experiments, 2 × 10^4 HIV-infected mLCs or mDCs were cocultured with 2 × 10^6 allogeneic CD4$^+$ T cells for 12 days, and supernatants were harvested every third day and examined for HIV p24 protein content by ELISA (ZeptoMetrix) according to the manufacturer's instructions.

Epithelial sheets were obtained from suction blister roofs from HIV-negative healthy donors. For infection of epithelial tissue explants, 50 μl droplets containing HIV-1Ba-L at a 1/100 final dilution were placed on the inside surfaces of sterile plastic culture dish covers, as described previously (Kawamura et al., 2000). Explants were draped over droplets with the basal epithelial cell surface facing downward. Virus and explants were incubated together in this manner at 37°C in a humidified 5% CO_2 environment for 2 hr. Explants were washed in three separate wells in 6-well plates containing sterile PBS and then floated with the basal epithelial cell sides down in 12-well plates containing 2 ml of complete medium, without exogenous stimulants or cytokines. The emigrating cells from the epidermal sheets were collected 3 days after the HIV exposure. In some experiments, epidermal cell suspensions were prepared by limited trypsinization of epidermal sheets, as described previously (Miller et al., 2011a).

Pseudotyped Virus Infection and Luciferase Assay

To prepare pseudotyped viruses with Env from either HIV-1 (IIIB, JR-FL, or VSV), 293 T cells were cotransfected with the Env expression plasmid DNA, pLET, pJRFLenv, or pMD.G, respectively, and with pNLLuc (an Env-defective HIV-1NL4-3 carrying the luciferase gene) as described previously (Sato et al., 2008). The culture supernatants were harvested and then filtrated to produce virus solutions at 48 hr posttransfection. To measure the infectivity of Env-pseudotyped virus, mLCs were incubated with JR-FL Env- or IIIB Env-pseudotyped virus, containing 20 ng of p24CA, or VSV envelope glycoprotein-pseudotyped virus, containing 0.5 ng of p24CA, for 72 hr. The Picagene luciferase assay kit (Toyo Ink) was used to perform luciferase assays, following the manufacturer's protocols. Activity was measured with a 1420 ARVOSX multilabel counter (Perkin Elmer) and normalized to the protein content of each lysate, measured with a Coomassie (Bradford) protein assay kit (Pierce).

Flow Cytometry

Single-cell suspensions were stained using the following anti-human mAb: anti-CD83 (BD Biosciences-PharMingen), anti-CD86 (BD Biosciences-PharMingen), anti-CD4 (Beckman Coulter), anti-CCR5 (R&D), anti-DC-sign (R&D), anti-CCR7 (R&D) directly conjugated to FITC, anti-langerin (Immunotech) directly conjugated to PE, and anti-CD11c (Becton Dickinson) directly conjugated to allophycocyanin. Cells were incubated with Abs for 30 min at 4°C and then washed three times in staining buffer and examined by FACScaliber using propidium iodide (Sigma) to exclude the dead cells in the surface staining.

To specifically identify HIV- or HSV-infected cells on a single-cell level, HIV p24 or HSV gD intracellular staining was performed, respectively. Epidermal LCs, mLCs, and mDCs were collected at the indicated days after HIV exposure and then washed three times in staining buffer, and then incubated with 10 μg/ml allophycocyanin-conjugated mouse anti-human CD11c mAb, and with mLCs or without mDCs PE-conjugated mouse anti-human langerin mAb and for 30 min at 4°C. Cells were then washed three times in staining buffer and fixed and permeabilized with Cytofix/Cytoperm reagents (BD Biosciences-PharMingen) for 20 min at 4°C. Cells were then washed three times in Perm-Wash (BD Biosciences-PharMingen), incubated with FITC- or PE-conjugated mouse anti-HIV p24 mAb (Beckman Coulter) and/or FITC-conjugated mouse anti-HSV gD mAb (Argene) diluted for 30 min at 4°C, and washed three times in Perm-Wash, with the quantified numbers of HIV- or HSV-infected cells determined by FACScaliber.

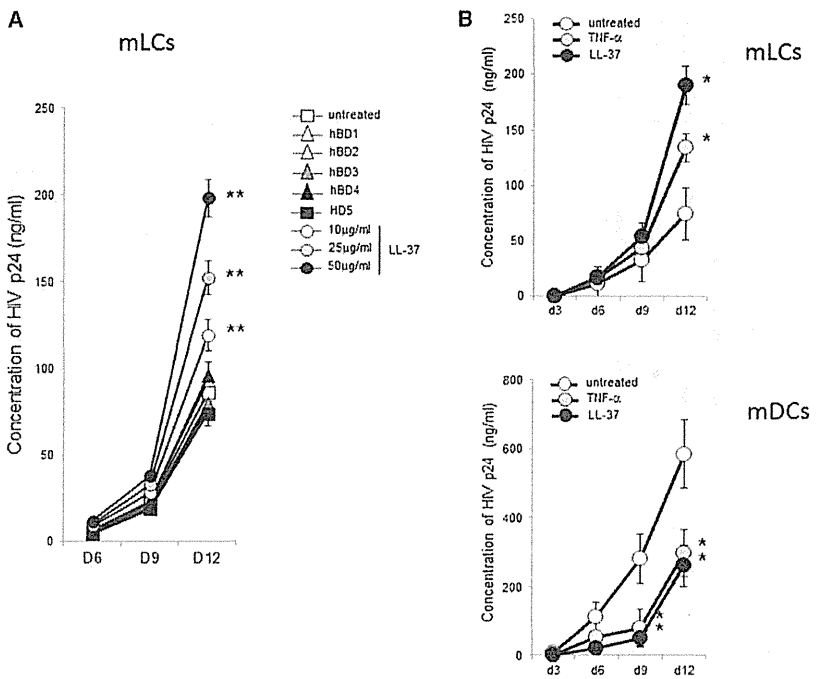

Figure 7. LL-37 Enhances HIV Transmission from mLCs to T Cells

mLCs (A) or mLCs and mDCs isolated from the same donor (B) were stimulated with the indicated AMPs or rhTNF-α 24 hr prior to HIV exposure. HIV-infected mLCs or mDCs were cocultured with allogeneic $CD4^+$ T cells, and p24 protein levels in culture supernatants were assessed by ELISA on the indicated days. Results are shown as means plus or minus SD (n = 3). *$p < 0.05$; **$p < 0.01$. All data shown represent at least two separate experiments.

RNA Interference Using siRNA

The delivery of siRNA into NHEKs was performed by DharmaFECT 3 siRNA Transfection Reagent (Dharmacon). Cells were transfected with siRNAs at a final concentration of 50 nM. The siRNAs used in this study were ON-TARGETplus nontargeting pool (Dharmacon #D 001810–10) for control siRNA and ON-TARGETplus SMARTpool siRNA Human CAMP (Dharmacon #L-019790–00) for LL-37 siRNA.

Real-Time Quantitative RT-PCR Analysis

Relative mRNA expression was determined by real-time PCR using an ABI PRISM 5500 Sequence Detection System (Applied Biosystems) with SYBR Green I dye (QIAGEN) according to the manufacturer's instructions. Total RNA was isolated using TRIzol (Invitrogen Life Technologies), and cDNA was synthesized using the SuperScript system (Invitrogen Life Technologies). Primers corresponding to human α defensin-5, defensin-6, human β defensin-1, β defensin-2, β defensin-3, β defensin-4, LL-37, and GAPDH were designed by Takara Bio, Inc. Cycle threshold numbers (Ct) were derived from the exponential phase of the PCR amplification. Fold differences in the expression of gene x in the cell populations y and z were derived by 2k, where k = (Ctx – CtG3PDH)y – (Ctx – CtG3PDH)z.

ELISA

NHEKs were exposed to live HSV-2 (10^6 PFU) or heat-inactivated HSV-2 for 1 hr, and then washed three times. Following culture in medium for the indicated days, the culture supernatants were collected after centrifugation and stored at −80°C for LL-37 and TNF-α measurement. The concentration of human LL-37 (Hycult biotechnology) and TNF-α (R&D Systems) in the culture supernatants was measured by ELISA. For measurement of HIV p24 protein levels, supernatants were collected, inactivated with Triton X-100 (Sigma-Aldrich; 2% final concentration), and kept frozen until measurements of HIV p24 protein levels were performed by ELISA (ZeptoMetrix).

Western Blot Analysis

Proteins of the cells were extracted using 15 min incubation in complete lysis buffer containing a protease inhibitor. Equal amounts of protein were separated by SDS-PAGE and transferred onto a transfer membrane (Daiichikagaku). Western blot was performed in order to detect hCAP18 (2.0 μg/ml, Abcam), KLK5 (2.0 μg/ml, R&D Systems), LL-37 (2.0 μg/ml, Santa Cruz), A3G (2.5 μg/ml, Abcam), and SAMHD1 (2.0 μg/ml, Abcam). Blots were incubated with the HRP-linked secondary antibody. Analyses were performed using the HRP western blot detection system (Pierce), and band intensities were calculated using ImageJ software.

Statistical Analyses

Significant differences between experimental groups were analyzed by Student's t test (one-tailed). p values less than 0.05 were considered significant.

Study Approval

The Institutional Review Board of the University Hospital (University of Yamanashi, Yamanashi, Japan) approved the acquisition of human tissues, and informed consent was obtained from all skin donors.

SUPPLEMENTAL INFORMATION

Supplemental Information includes five figures and can be found with this article at http://dx.doi.org/10.1016/j.chom.2012.12.002.

ACKNOWLEDGMENTS

We would like to thank Kazutoshi Harada and Naotaka Shibagaki for their helpful discussions; Miyuki Ogino and Naoko Misawa for technical assistance; and Takashi Fujita, Keizo Tomonaga, and Klaus Strebel for providing reagents. These studies were supported in part by a grant from the Ministry of Education and Science of the Japanese Government. Y.O. performed experiments and analyzed data. T.K. directed and performed experiments, analyzed data, and wrote the manuscript. T.M. and R.A. performed experiments and analyzed data. P.G. and A.Y. performed experiments. K.M. contributed analytical tools. K.Y. and Y.K. codirected experiments. A.B. codirected experiments and wrote the manuscript. S.S. codirected experiments.

Received: June 28, 2012
Revised: September 18, 2012
Accepted: December 12, 2012
Published: January 16, 2013

REFERENCES

Auvert, B., Taljaard, D., Lagarde, E., Sobngwi-Tambekou, J., Sitta, R., and Puren, A. (2005). Randomized, controlled intervention trial of male circumcision for reduction of HIV infection risk: the ANRS 1265 Trial. PLoS Med. 2, e298. http://dx.doi.org/10.1371/journal.pmed.0020298.

Bailey, R.C., Moses, S., Parker, C.B., Agot, K., Maclean, I., Krieger, J.N., Williams, C.F., Campbell, R.T., and Ndinya-Achola, J.O. (2007). Male circumcision for HIV prevention in young men in Kisumu, Kenya: a randomised controlled trial. Lancet *369*, 643–656.

Bergman, P., Walter-Jallow, L., Broliden, K., Agerberth, B., and Söderlund, J. (2007). The antimicrobial peptide LL-37 inhibits HIV-1 replication. Curr. HIV Res. *5*, 410–415.

Cameron, D.W., Simonsen, J.N., D'Costa, L.J., Ronald, A.R., Maitha, G.M., Gakinya, M.N., Cheang, M., Ndinya-Achola, J.O., Piot, P., Brunham, R.C., et al. (1989). Female to male transmission of human immunodeficiency virus type 1: risk factors for seroconversion in men. Lancet *2*, 403–407.

Cunningham, A.L., Turner, R.R., Miller, A.C., Para, M.F., and Merigan, T.C. (1985). Evolution of recurrent herpes simplex lesions. An immunohistologic study. J. Clin. Invest. *75*, 226–233.

de Jong, M.A., de Witte, L., Oudhoff, M.J., Gringhuis, S.I., Gallay, P., and Geijtenbeek, T.B. (2008). TNF-alpha and TLR agonists increase susceptibility to HIV-1 transmission by human Langerhans cells ex vivo. J. Clin. Invest. *118*, 3440–3452.

de Jong, M.A., de Witte, L., Taylor, M.E., and Geijtenbeek, T.B. (2010). Herpes simplex virus type 2 enhances HIV-1 susceptibility by affecting Langerhans cell function. J. Immunol. *185*, 1633–1641.

de Witte, L., Nabatov, A., Pion, M., Fluitsma, D., de Jong, M.A., de Gruijl, T., Piguet, V., van Kooyk, Y., and Geijtenbeek, T.B. (2007). Langerin is a natural barrier to HIV-1 transmission by Langerhans cells. Nat. Med. *13*, 367–371.

Fahrbach, K.M., Barry, S.M., Anderson, M.R., and Hope, T.J. (2010). Enhanced cellular responses and environmental sampling within inner foreskin explants: implications for the foreskin's role in HIV transmission. Mucosal Immunol. *3*, 410–418.

Fleming, D.T., and Wasserheit, J.N. (1999). From epidemiological synergy to public health policy and practice: the contribution of other sexually transmitted diseases to sexual transmission of HIV infection. Sex. Transm. Infect. *75*, 3–17.

Galvin, S.R., and Cohen, M.S. (2004). The role of sexually transmitted diseases in HIV transmission. Nat. Rev. Microbiol. *2*, 33–42.

Ganor, Y., Zhou, Z., Tudor, D., Schmitt, A., Vacher-Lavenu, M.C., Gibault, L., Thiounn, N., Tomasini, J., Wolf, J.P., and Bomsel, M. (2010). Within 1 h, HIV-1 uses viral synapses to enter efficiently the inner, but not outer, foreskin mucosa and engages Langerhans-T cell conjugates. Mucosal Immunol. *3*, 506–522.

Gray, R.H., Kigozi, G., Serwadda, D., Makumbi, F., Watya, S., Nalugoda, F., Kiwanuka, N., Moulton, L.H., Chaudhary, M.A., Chen, M.Z., et al. (2007). Male circumcision for HIV prevention in men in Rakai, Uganda: a randomised trial. Lancet *369*, 657–666.

Gringhuis, S.I., van der Vlist, M., van den Berg, L.M., den Dunnen, J., Litjens, M., and Geijtenbeek, T.B. (2010). HIV-1 exploits innate signaling by TLR8 and DC-SIGN for productive infection of dendritic cells. Nat. Immunol. *11*, 419–426.

Grivel, J.C., Shattock, R.J., and Margolis, L.B. (2011). Selective transmission of R5 HIV-1 variants: where is the gatekeeper? J. Transl. Med. *9*(*Suppl 1*), S6.

Haase, A.T. (2010). Targeting early infection to prevent HIV-1 mucosal transmission. Nature *464*, 217–223.

Hrecka, K., Hao, C., Gierszewska, M., Swanson, S.K., Kesik-Brodacka, M., Srivastava, S., Florens, L., Washburn, M.P., and Skowronski, J. (2011). Vpx relieves inhibition of HIV-1 infection of macrophages mediated by the SAMHD1 protein. Nature *474*, 658–661.

Hu, J., Gardner, M.B., and Miller, C.J. (2000). Simian immunodeficiency virus rapidly penetrates the cervicovaginal mucosa after intravaginal inoculation and infects intraepithelial dendritic cells. J. Virol. *74*, 6087–6095.

Kawamura, T., Cohen, S.S., Borris, D.L., Aquilino, E.A., Glushakova, S., Margolis, L.B., Orenstein, J.M., Offord, R.E., Neurath, A.R., and Blauvelt, A. (2000). Candidate microbicides block HIV-1 infection of human immature Langerhans cells within epithelial tissue explants. J. Exp. Med. *192*, 1491–1500.

Kawamura, T., Qualbani, M., Thomas, E.K., Orenstein, J.M., and Blauvelt, A. (2001). Low levels of productive HIV infection in Langerhans cell-like dendritic cells differentiated in the presence of TGF-beta1 and increased viral replication with CD40 ligand-induced maturation. Eur. J. Immunol. *31*, 360–368.

Kawamura, T., Gulden, F.O., Sugaya, M., McNamara, D.T., Borris, D.L., Lederman, M.M., Orenstein, J.M., Zimmerman, P.A., and Blauvelt, A. (2003). R5 HIV productively infects Langerhans cells, and infection levels are regulated by compound CCR5 polymorphisms. Proc. Natl. Acad. Sci. USA *100*, 8401–8406.

Kawamura, T., Kurtz, S.E., Blauvelt, A., and Shimada, S. (2005). The role of Langerhans cells in the sexual transmission of HIV. J. Dermatol. Sci. *40*, 147–155.

Kawamura, T., Koyanagi, Y., Nakamura, Y., Ogawa, Y., Yamashita, A., Iwamoto, T., Ito, M., Blauvelt, A., and Shimada, S. (2008). Significant virus replication in Langerhans cells following application of HIV to abraded skin: relevance to occupational transmission of HIV. J. Immunol. *180*, 3297–3304.

Klotman, M.E., and Chang, T.L. (2006). Defensins in innate antiviral immunity. Nat. Rev. Immunol. *6*, 447–456.

Klotman, M.E., Rapista, A., Teleshova, N., Micsenyi, A., Jarvis, G.A., Lu, W., Porter, E., and Chang, T.L. (2008). Neisseria gonorrhoeae-induced human defensins 5 and 6 increase HIV infectivity: role in enhanced transmission. J. Immunol. *180*, 6176–6185.

Koyanagi, Y., Tanaka, Y., Kira, J., Ito, M., Hioki, K., Misawa, N., Kawano, Y., Yamasaki, K., Tanaka, R., Suzuki, Y., et al. (1997). Primary human immunodeficiency virus type 1 viremia and central nervous system invasion in a novel hu-PBL-immunodeficient mouse strain. J. Virol. *71*, 2417–2424.

Laguette, N., Sobhian, B., Casartelli, N., Ringeard, M., Chable-Bessia, C., Ségéral, E., Yatim, A., Emiliani, S., Schwartz, O., and Benkirane, M. (2011). SAMHD1 is the dendritic- and myeloid-cell-specific HIV-1 restriction factor counteracted by Vpx. Nature *474*, 654–657.

Lederman, M.M., Veazey, R.S., Offord, R., Mosier, D.E., Dufour, J., Mefford, M., Piatak, M., Jr., Lifson, J.D., Salkowitz, J.R., Rodriguez, B., et al. (2004). Prevention of vaginal SHIV transmission in rhesus macaques through inhibition of CCR5. Science *306*, 485–487.

Lederman, M.M., Offord, R.E., and Hartley, O. (2006). Microbicides and other topical strategies to prevent vaginal transmission of HIV. Nat. Rev. Immunol. *6*, 371–382.

Levinson, P., Kaul, R., Kimani, J., Ngugi, E., Moses, S., MacDonald, K.S., Broliden, K., and Hirbod, T.; Kibera HIV Study Group. (2009). Levels of innate immune factors in genital fluids: association of alpha defensins and LL-37 with genital infections and increased HIV acquisition. AIDS *23*, 309–317.

Liu, R., Paxton, W.A., Choe, S., Ceradini, D., Martin, S.R., Horuk, R., MacDonald, M.E., Stuhlmann, H., Koup, R.A., and Landau, N.R. (1996). Homozygous defect in HIV-1 coreceptor accounts for resistance of some multiply-exposed individuals to HIV-1 infection. Cell *86*, 367–377.

Miller, C.J., Johnson, S.L., Kwapil, T.R., and Carver, C.S. (2011a). Three studies on self-report scales to detect bipolar disorder. J. Affect. Disord. *128*, 199–210.

Miller, C.J., Rose, A.L., and Waite, T.D. (2011b). Phthalhydrazide chemiluminescence method for determination of hydroxyl radical production: modifications and adaptations for use in natural systems. Anal. Chem. *83*, 261–268.

Morizane, S., Yamasaki, K., Kabigting, F.D., and Gallo, R.L. (2010). Kallikrein expression and cathelicidin processing are independently controlled in keratinocytes by calcium, vitamin D(3), and retinoic acid. J. Invest. Dermatol. *130*, 1297–1306.

Ogawa, Y., Kawamura, T., Kimura, T., Ito, M., Blauvelt, A., and Shimada, S. (2009). Gram-positive bacteria enhance HIV-1 susceptibility in Langerhans cells, but not in dendritic cells, via Toll-like receptor activation. Blood *113*, 5157–5166.

Ong, P.Y., Ohtake, T., Brandt, C., Strickland, I., Boguniewicz, M., Ganz, T., Gallo, R.L., and Leung, D.Y. (2002). Endogenous antimicrobial peptides and skin infections in atopic dermatitis. N. Engl. J. Med. *347*, 1151–1160.

Pion, M., Granelli-Piperno, A., Mangeat, B., Stalder, R., Correa, R., Steinman, R.M., and Piguet, V. (2006). APOBEC3G/3F mediates intrinsic resistance of monocyte-derived dendritic cells to HIV-1 infection. J. Exp. Med. *203*, 2887–2893.

Quiñones-Mateu, M.E., Lederman, M.M., Feng, Z., Chakraborty, B., Weber, J., Rangel, H.R., Marotta, M.L., Mirza, M., Jiang, B., Kiser, P., et al. (2003). Human epithelial beta-defensins 2 and 3 inhibit HIV-1 replication. AIDS *17*, F39–F48.

Reece, J.C., Handley, A.J., Anstee, E.J., Morrison, W.A., Crowe, S.M., and Cameron, P.U. (1998). HIV-1 selection by epidermal dendritic cells during transmission across human skin. J. Exp. Med. *187*, 1623–1631.

Sato, K., Aoki, J., Misawa, N., Daikoku, E., Sano, K., Tanaka, Y., and Koyanagi, Y. (2008). Modulation of human immunodeficiency virus type 1 infectivity through incorporation of tetraspanin proteins. J. Virol. *82*, 1021–1033.

Shattock, R.J., and Moore, J.P. (2003). Inhibiting sexual transmission of HIV-1 infection. Nat. Rev. Microbiol. *1*, 25–34.

Spira, A.I., Marx, P.A., Patterson, B.K., Mahoney, J., Koup, R.A., Wolinsky, S.M., and Ho, D.D. (1996). Cellular targets of infection and route of viral dissemination after an intravaginal inoculation of simian immunodeficiency virus into rhesus macaques. J. Exp. Med. *183*, 215–225.

Sun, L., Finnegan, C.M., Kish-Catalone, T., Blumenthal, R., Garzino-Demo, P., La Terra Maggiore, G.M., Berrone, S., Kleinman, C., Wu, Z., Abdelwahab, S., et al. (2005). Human beta-defensins suppress human immunodeficiency virus infection: potential role in mucosal protection. J. Virol. *79*, 14318–14329.

Theodore, T.S., Englund, G., Buckler-White, A., Buckler, C.E., Martin, M.A., and Peden, K.W. (1996). Construction and characterization of a stable full-length macrophage-tropic HIV type 1 molecular clone that directs the production of high titers of progeny virions. AIDS Res. Hum. Retroviruses *12*, 191–194.

Wald, A., and Link, K. (2002). Risk of human immunodeficiency virus infection in herpes simplex virus type 2-seropositive persons: a meta-analysis. J. Infect. Dis. *185*, 45–52.

Yamasaki, K., Schauber, J., Coda, A., Lin, H., Dorschner, R.A., Schechter, N.M., Bonnart, C., Descargues, P., Hovnanian, A., and Gallo, R.L. (2006). Kallikrein-mediated proteolysis regulates the antimicrobial effects of cathelicidins in skin. FASEB J. *20*, 2068–2080.

Yamasaki, K., Di Nardo, A., Bardan, A., Murakami, M., Ohtake, T., Coda, A., Dorschner, R.A., Bonnart, C., Descargues, P., Hovnanian, A., et al. (2007). Increased serine protease activity and cathelicidin promotes skin inflammation in rosacea. Nat. Med. *13*, 975–980.

Zaitseva, M., Blauvelt, A., Lee, S., Lapham, C.K., Klaus-Kovtun, V., Mostowski, H., Manischewitz, J., and Golding, H. (1997). Expression and function of CCR5 and CXCR4 on human Langerhans cells and macrophages: implications for HIV primary infection. Nat. Med. *3*, 1369–1375.

Zhang, Z.Q., Schuler, T., Cavert, W., Notermans, D.W., Gebhard, K., Henry, K., Havlir, D.V., Günthard, H.F., Wong, J.K., Little, S., et al. (1999). Reversibility of the pathological changes in the follicular dendritic cell network with treatment of HIV-1 infection. Proc. Natl. Acad. Sci. USA *96*, 5169–5172.

Zhou, Z., Barry de Longchamps, N., Schmitt, A., Zerbib, M., Vacher-Lavenu, M.C., Bomsel, M., and Ganor, Y. (2011). HIV-1 efficient entry in inner foreskin is mediated by elevated CCL5/RANTES that recruits T cells and fuels conjugate formation with Langerhans cells. PLoS Pathog. *7*, e1002100. http://dx.doi.org/10.1371/journal.ppat.1002100.

Zhu, T., Mo, H., Wang, N., Nam, D.S., Cao, Y., Koup, R.A., and Ho, D.D. (1993). Genotypic and phenotypic characterization of HIV-1 patients with primary infection. Science *261*, 1179–1181.

Zhu, J., Hladik, F., Woodward, A., Klock, A., Peng, T., Johnston, C., Remington, M., Magaret, A., Koelle, D.M., Wald, A., and Corey, L. (2009). Persistence of HIV-1 receptor-positive cells after HSV-2 reactivation is a potential mechanism for increased HIV-1 acquisition. Nat. Med. *15*, 886–892.

Journal of Virology

Deep-Sequencing Analysis of the Association between the Quasispecies Nature of the Hepatitis C Virus Core Region and Disease Progression

Mika Miura, Shinya Maekawa, Shinichi Takano, Nobutoshi Komatsu, Akihisa Tatsumi, Yukiko Asakawa, Kuniaki Shindo, Fumitake Amemiya, Yasuhiro Nakayama, Taisuke Inoue, Minoru Sakamoto, Atsuya Yamashita, Kohji Moriishi and Nobuyuki Enomoto

J. Virol. **2013, 87(23):12541. DOI: 10.1128/JVI.00826-13.**
Published Ahead of Print 14 August 2013.

JVI
Journals.ASM.org

Deep-Sequencing Analysis of the Association between the Quasispecies Nature of the Hepatitis C Virus Core Region and Disease Progression

Mika Miura,[a] Shinya Maekawa,[a] Shinichi Takano,[a] Nobutoshi Komatsu,[a] Akihisa Tatsumi,[a] Yukiko Asakawa,[a] Kuniaki Shindo,[a] Fumitake Amemiya,[a] Yasuhiro Nakayama,[a] Taisuke Inoue,[a] Minoru Sakamoto,[a] Atsuya Yamashita,[b] Kohji Moriishi,[b] Nobuyuki Enomoto[a]

First Department of Internal Medicine, Faculty of Medicine, University of Yamanashi, Shimokato, Chuo, Yamanashi, Japan[a]; Department of Microbiology, University of Yamanashi, Shimokato, Chuo, Yamanashi, Japan[b]

Variation of core amino acid (aa) 70 of hepatitis C virus (HCV) has been shown recently to be closely correlated with liver disease progression, suggesting that the core region might be present as a quasispecies during persistent infection and that this quasispecies nature might have an influence on the progression of disease. In our investigation, the subjects were 79 patients infected with HCV genotype 1b (25 with chronic hepatitis [CH], 29 with liver cirrhosis [LC], and 25 with hepatocellular carcinoma [HCC]). Deep sequencing of the HCV core region was carried out on their sera by using a Roche 454 GS Junior pyrosequencer. Based on a plasmid containing a cloned HCV sequence (pCV-J4L6S), the background error rate associated with pyrosequencing, including the PCR procedure, was calculated as 0.092 ± 0.005/base. Deep sequencing of the core region in the clinical samples showed a mixture of "mutant-type" Q/H and "wild-type" R at the core aa 70 position in most cases (71/79 [89.9%]), and the ratio of mutant residues to R in the mixture increased as liver disease advanced to LC and HCC. Meanwhile, phylogenetic analysis of the almost-complete core region revealed that the HCV isolates differed genetically depending on the mutation status at core aa 70. We conclude that the core aa 70 mixture ratio, determined by deep sequencing, reflected the status of liver disease, demonstrating a significant association between core aa 70 and disease progression in CH patients infected with HCV genotype 1b.

Hepatitis C virus (HCV)-related liver disease gradually advances from chronic hepatitis (CH) to liver cirrhosis (LC) and to hepatocellular carcinoma (HCC) over 20 to 30 years (1). However, the rates of disease progression differ: some patients develop HCC over several years, while others show persistently normal alanine aminotransferase (PNALT) levels for decades, and the cause of the difference remains poorly understood.

The involvement of viral and host factors in the progression of liver disease and hepatocarcinogenesis is complex (2). With regard to viral factors, the relationship between the viral core region and disease progression in HCV genotype 1b infection has attracted clinical attention. Specifically, it has been reported that the core amino acid (aa) 70 residue, identified as a variable related to the outcome of interferon (IFN) therapy (3), is closely associated with the progression of hepatitis and hepatocarcinogenesis in Japan and North America (4–7). Those previous studies and our own have reported that core aa 70 variation is strongly linked to carcinogenesis and that substitutions in the core aa 70 region aggravate hepatitis and heighten the risk of hepatocarcinogenesis during the clinical course, corroborating the relationship between the status of the core region and disease progression (8, 9).

With regard to host factors, a genomewide association study (GWAS) has recently shown that single nucleotide polymorphisms (SNPs) around the interleukin 28B (IL28B) gene (rs12979860 and rs8099917), encoding the type III IFN IFN-λ3, are strongly correlated with the outcomes of therapy with pegylated IFN-α plus ribavirin for chronic hepatitis C (CH-C) (10–13). Interestingly, in contrast to the core region, consensus has not been reached as to the relationship between disease progression and the IL28B SNP, which is associated with IFN resistance (14–17). Previously, we reported that there was no correlation between the onset of HCC and the IL28B SNP (9). However, it was reported that the IL28B rs8099917 TG/GG allele was markedly correlated with the presence of Q (glutamine) or H (histidine) instead of the R (arginine) residue at core aa 70, while the IL28B rs8099917 TT allele was correlated with core aa 70R (8). Moreover, the core amino acid R70Q/H change occurs more often in patients with IL28B rs8099917 TG/GG than in those with IL28B rs8099917 TT (9). In this manner, the contributions of the core aa 70 residue and the IL28B SNP, which were found to be IFN sensitivity factors, to the progression of liver disease have gradually been elucidated.

HCV exists in a host as a swarm of variants, known as a "quasispecies," and this quasispecies nature has been considered to play a critical role in pathogenesis (18). However, detailed analysis has been technically difficult, and the clinical significance has not been clarified in detail thus far. Considering the observation of core aa 70 gene changes over time, it is assumed that a variety of core aa 70 isolates may exist as a quasispecies, and this could be related to pathogenesis as described above.

Recently, deep-sequencing technology has advanced rapidly and has enabled us to analyze viral quasispecies in association with the status of the disease (19–22). In this study, we investigated how the quasispecies of the HCV core gene, either at the hot spot of the core aa 70 residue or in the almost-entire core gene, is created and is involved in disease progression in patients with CH-C.

Received 28 March 2013 Accepted 7 August 2013
Published ahead of print 14 August 2013
Address correspondence to Shinya Maekawa, maekawa@yamanashi.ac.jp.
Supplemental material for this article may be found at http://dx.doi.org/10.1128/JVI.00826-13.

doi:10.1128/JVI.00826-13